



**Politecnico  
di Torino**

# Politecnico di Torino

Master's Degree in Mechanical Engineering

Graduation Session of July 2023

Master's Degree Thesis

## **Cementitious based composite materials for thermal energy storage applications**

Supervisors:

Prof. Eliodoro Chiavazzo

Prof. Matteo Pavese

Prof. Luca Lavagna

Candidate:

Matteo Barbatelli

Academic Year 2022/2023

# Abstract

Over the last century the exploitation of resources in the energy production generated clear and indisputable devastation in the ecosystem, such as global warming or combustion and dispersion of fossil fuels in the environment. The aim of the researches conducted in the last period is both to capitalize on renewable resources to avoid the diffusion of  $CO_2$  and both to cope with the mismatch of energy production and its demand. In this scenario, Sorption Thermal Energy Storage, even though still being a technology little known, appears to play a key role in the renewable energy sources system. This technology allows to stock an high amount of energy during the warm season and then releasing it when is needed, without significant losses.

The sorption phenomena is based on the interaction between a sorbent and a sorbate that undergo a reversible adsorption-desorption reaction which allows to stock energy when the two substances are kept separated and to release it when they are brought together. The researches in the last period moved on the investigation of the suitable couple of materials sorbent-sorbate that grant the higher energy density release combined with the lower affordable cost. Composite materials result to be an adequate candidate that permit to store an elevate amount of energy without significant losses.

The aim of this thesis is to produce a robust and low-cost composite material by using as host matrix the common Portland cement and accommodating inside some hygroscopic salts, precisely Magnesium Sulfate ( $MgSO_4$ ) and Calcium Chloride ( $CaCl_2$ ). The choice of the cement as matrix for the composite material is due to his porous morphology, which permit to accommodate salts inside it, to his uncomplicated availability on our planet and to his relative low cost with respect to the common sorbents employed so far as matrix.

In the work are showed two methods to produce this composite material: a dry impregnation of saturated salt solution inside a white pure cement basis and a new proposed in situ synthesis where the powder cement is directed mixed with the saturated salt solution rather than pure water.

The samples produced characterized by the higher estimated salt fraction within are tested thermally firstly assembling a preliminary thermal test in the university laboratory. The most promising ones are investigated at the National Institute of Metrological Research (INRiM) with the purpose of obtain the sorption parameters to classify the composite material. Two absorption isotherms are plotted after testing the sample respectively at  $30^\circ C$  and  $50^\circ C$  and the most important properties, i.e. water uptake, isosteric heat and energy density are calculated. Only the samples produced with sulfate magnesium allows a complete estimation of the properties, as a matter of fact the intrinsic deliquescence behaviour of calcium chloride inhibit a correct sorption test in the climatic chamber. The best sample results to be an in situ synthesized with sulfate magnesium and impregnated two times with the same salt. From the preliminary thermal test it reached a maximum energy density of  $0.15 \text{ GJ}/m^3$ , while in the sorption analysis reached a value of  $0.18 \text{ GJ}/m^3$ , when the desorption temperature is  $150^\circ C$ .

# Content

<b>Chapter 1. Introduction.....</b>	<b>6</b>
<b>Chapter 2. Sorption Heat Storage.....</b>	<b>7</b>
2.1 Sensible Heat Storage.....	8
2.2 Latent Heat Storage.....	9
2.3 Sorption Thermal Energy Storage (STES).....	9
2.4 Materials for sorption heat storage.....	12
2.4.1 liquid absorption.....	12
2.4.2 solid adsorption.....	13
2.4.3 solid absorption.....	15
2.4.4 composite materials for sorption heat storage.....	19
2.4.5 cementitious composite materials.....	19
2.5 storage systems.....	20
2.6 thermodynamic cycle.....	22
<b>Chapter 3. Cement: fundamentals and main features.....</b>	<b>23</b>
3.1 cement production.....	23
3.2 cement composition.....	25
3.3 porosity.....	25
3.4 bleeding .....	26
<b>Chapter 4. Materials and Procedures.....</b>	<b>27</b>
4.1 matrix preparation.....	27
4.2 impregnation.....	29
4.3 in situ.....	31
4.4 in situ impregnated.....	33
4.5 preliminary thermal test.....	33
4.6 sorption analysis.....	35

4.7 the Brunauer–Emmett–Teller (BET) modeling.....	36
4.8 sorption properties evaluation.....	38
<b>Chapter 5. Result and Discussion.....</b>	<b>40</b>
5.1 salt content.....	40
5.2 Preliminary thermal analysis .....	43
5.3 sorption test.....	45
5.3.1 BET fitting results.....	45
5.3.2 sorption properties evaluation.....	47
5.3.3 preliminary cost analysis.....	51
<b>Chapter 6. Conclusion.....</b>	<b>53</b>
<b>Bibliography</b>	

## List of Figure

Figure 2.1 - Schematic representation of sorption phenomena.....	9
Figure 2.2 - 5 type of isotherms (BET theory) based on the morphology of the solid.....	10
Figure 2.3 - Energy densities for the different TES mechanisms, among which the STES has the highest energy density, followed by the latent heat storage system. With a high energy density, the volume required to store the energy should be reduced.....	11
Figure 2.4 - Energy storage densities of sorption materials.....	17
Figure 2.5 - storage capacity cost in relation to charging temperatures for the sorbent materials (21).....	18
Figure 2.6 - schematic representation of an open thermal systems.....	20
Figure 2.7 - schematic representation of closed thermal systems.....	21
Figure 2.8 - Working cycle of an adsorption heat storage.....	22
Figure 3.1 - grafic scheme of the cement production.....	24
Figure 5.1 - BET model fitting of experimental data for the different samples at 50°C and 30°C....	46
Figure 5.2 - Characteristic sorption curve for the samples.....	47

Figure 5.3 - Adsorption isotherms at 10°C, 30°C, 35°C, 40°C, 50°C, 90°C .....48

Figure 5.4 - Clapeyron cycle for the samples. Working temperatures:  $T_w=10^\circ\text{C}$ ;  $T_s=30^\circ\text{C}$ ;  $T_A=40^\circ\text{C}$ ;  $T_C=150^\circ\text{C}$ .....49

## List of Table

Table 4.1– Experimental water uptake of the samples in the climatic chamber.....37

Table 5.1 – Levels of salt fraction and density obtained in the production of the different samples.....43

Table 5.2 – Energy density obtained for the impregnated samples in the preliminary thermal test.....44

Table 5.3 – Energy density obtained for the in-situ samples in the preliminary thermal test.....44

Table 5.4 – Parameters for the BET fitting procedure.....46

Table 5.5 – Parameters of the fitting function curve for the samples.....47

Table 5.6 – Estimated sorption parameters.....50

Table 5.7 – Estimated energy density.....51

Table 5.8 – Comparison between the samples produced and other materials from literature in terms of KPI and energy density.....52

# 1. Introduction

Over the last years the humanity has moved towards what is defined 'energy crisis', term used to indicate a ever-increasing energy demand accompanied by a continuous depletion of traditional resources (1). The demographic growth of the population occurred in the last period is the cause that led to the rise of energy demand around the world, bringing to a greater exploitation of the available resources. Recent reports forecast further increase in the energy demand of about 18% for already industrialized countries and of 71% for developing countries until 2040 (2).

To face this ever-increasing energy demand the conventional resources employed until now follow the criterion of being low-cost, but the drawback is that they have negative consequences in the environment such as air and water pollution, ozone layer depletion, habitat degradation, climate changing. One of the major responsible of the degradation of the ecosystem is the dependence that thermal power plants has on burning fossil fuels, which are the largest single source of global greenhouse-gas emissions. The fossil fuel era began near the end of the 19<sup>th</sup> century and the exploitation of this resource has risen until nowadays, when it is estimated that about 70% of the world's power is created by burning it (3). The combustion of fossil fuels liberates carbon dioxide (CO<sub>2</sub>), which is one of the so called 'greenhouse gases'. The prolonged dispersion of this gas in the environment during the years is the reason of the damaging of the ecosystem, changing climate, ozone layer depletion, pollution.

The need to cut greenhouse gases mission is well recognized in the present time, the world community pushes new researches in the direction to try new methods to produce energy with renewable resources. The heating and cooling industry play a key role in the building of new systems no more based on burning fossil fuels, since global power consumption, including transportation, industry, residential and commercial use account for the most widespread fields of energy demand.

Although the direction towards the research in renewable resources is traced, several are the obstacle to overcome. One of these is the mismatch between availability of the source, for instance the sunlight abundant in the warm season, and the demand of energy which is higher in the cold season. In this scenario energy storage is one of the possible solution to cope with the discrepancy between energy supply and demand. The future of the renewable resources will be dominated by the potential of intermittent and distributed energy production technology with benefits in the energy grid flexibility and safety. Thus the greatest research efforts are based in sorption thermal energy storage (STES) systems with the aim of gradually mitigating the greenhouse gases emission plant in an economical and sustainable manner.

This paper presents a brief introduction of the common STES systems, especially accompanied by solar-thermal electricity generation by means of solar panel, a technology that is becoming increasingly popular and allows to store thermal energy in the long and medium period. Aim of this work is therefore to produce a robust and low-cost composite material that can guarantee excellent performance in the field of storing and releasing thermal energy and can represent a solid candidate to be exploited in the STES technology.

## 2. Sorption Heat Storage

Thermal Energy storage (TES) allows to cope with the mismatch of time between energy production and energy demand, because this type of systems offer the possibility to store energy, in the form of heat or cold, in a suitable storage medium for a certain period of time without significant losses. Technology such as solar collectors are only productive during the day when domestic heating demand is at its lowest, and so in the evening when the demand increases the heat is no longer available (4).

The typical TES cycle involves three phases: charge, storage, discharge. At first it is necessary to provide heat in order to charge the system (desorption process), for instance in the summer period the exploitation of solar collectors allow to collect radiation energy from the sun and to convert it in exploitable energy. The phase of storage is the crucial one, indeed the amount of storable and retrievable heat depends for the most part on the employed storage means and on the thermal losses. Then it is possible to release the stored energy at any future time when there is a need, as it happens in the winter season, satisfying the discrepancy between energy production and demand.

In the last century several studies are pointed in the direction to find the best compromise of system and storage medium in order to find an effective way to exploit renewable energy sources and to reduce the environmental impact of heating and cooling.

In the design of a solar thermal energy storage system three parameters needs to be considered: technical properties, cost effectiveness and environmental impact (5).

The technical properties that need to be excellent in order to have an optimum feasibility of the thermal energy storage are:

- High thermal storage capacity (sensible heat, in order to minimize volume of the system and maximize the efficiency)
- Good heat transfer rate between the heat storage material and heat transfer fluid, to ensure that thermal energy can be released/absorbed at the required speed
- The storage material needs to have good stability to avoid chemical and mechanical degradation after a certain number of thermal cycles

The cost effectiveness impacts on the payoff period of the investment, so the high influence on the price of a storage system is given by the cost of the storage material, the material of the heat exchanger and the land cost.

The criteria that should be considered for the environmental impact are: the operation strategy, the integration to a specific power plant.

It is possible to differentiate three different systems: sensible heat storage (SHS), latent heat storage (LHS) and sorption thermal energy storage (STES)

## 2.1 Sensible heat storage (SHS)

The working principle of SHS consists in storing thermal energy by increasing or the temperature of a liquid or solid storage medium, in order to store heat and then decreasing it to release thermal energy when it is needed. Hence, the amount of storable heat  $Q$  is established following this rule:

$$Q = \rho \cdot V \cdot c_p \cdot \Delta T = M \cdot c_p \cdot \Delta T$$

As consequence, thermal energy stored depends on the specific heat capacity  $c_p$ , density  $\rho$ , storage volume  $V$  of the storage medium and temperature difference  $\Delta T$  experienced by the material during charging.

The most commonly used materials for SHS systems are solid-state, liquid-state or salt mixtures. The main characteristic of solid-state and liquid-state thermal storage materials are listed in the table below [A review of solar collectors and thermal energy storage in solar thermal], while the salt mixtures most worthy of notation are  $KNO_3$ ,  $LiNO_3$  and  $Ca(NO_3)_2$ . It is worth noting that the common advantage of the materials suitable for SHS is the low cost, ranging from 0.05 \$/kg to 5.00 \$/kg (5). However, seasonal sensible heat storage requires in general large volume to reduce thermal losses, because of its low energy density, resulting in high capital expenditure.

## 2.2 latent heat storage

The LHS systems take advantage of the property of releasing or absorbing thermal energy through a phase change (commonly named Phase Change Materials), depending on the latent heat of the storage medium. Unlike conventional (sensible) storage materials, PCM absorbs and release heat at a nearly constant temperature.

The energy that can be stored inside the PCM can be evaluated through this formula:

$$E = m \cdot L + m \cdot c_p \cdot \Delta T$$

The first term of the summation takes in account the transformation latent heat of the material,  $L$  [kJ/kg], while the second term includes a sensible heat amount due to the increase of the temperature.

Most of the current applications involve solid-liquid transition, even if also solid-solid and liquid-gas transition are taken in account. Exploiting also the material latent heat, PCM energy densities are higher than the ones of sensible heat storage materials. However, their commercialization is hindered by a number of challenges, such as a complex design is required to avoid conditions of low thermal conductivity of the material (for example the introduction of some fins can increase the conductivity) and risks of supercooling or segregation, index of low stability (the introduction of a nucleating agent can overcome the supercooling problem) (1).

## 2.3 sorption thermal energy storage (STES)

In STES the charging and discharge phase take place by means of a reaction between two components: a sorbent, which is typically a liquid or solid, and a sorbate, which is typically a vapor. During the charging process, an endothermic reaction occurs, and the sorbent and sorbate are separated. The two components can then be stored separately, ideally without energy losses. During the discharging process, sorbent and sorbate react producing an exothermic reaction that releases heat (6).

Sorption and thermochemical storage systems use a reversible physio-chemical phenomena to store energy:



A and B are the sorbent and sorbate material (Fig 2.1). The compound AB is called working pair or sorption couple. Under the influence of a heat supply it is split into chemical substances A and B through an endothermic dissociation reaction. The produced chemical substances, A and B, are capable of storing thermal energy in the form of the chemical potential energy and can be stored separately to achieve long period heat storage with little heat loss. When the reversible reaction occurs for the later heat utilization, compound AB is regenerated resulting from the synthesis reaction between substances A and B. As a result, the stored thermal energy is retrieved.

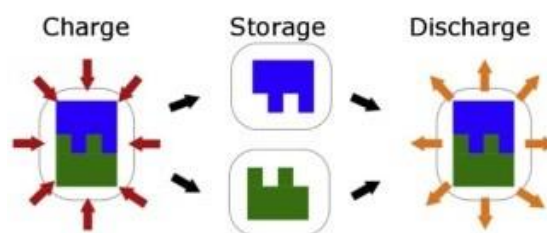


Fig 2.1 - Schematic representation of sorption phenomena

Sorption is a reaction that includes two mechanisms: absorption and adsorption. Absorption is defined as *the process of one material (absorbate) being retained by another (absorbent)*. It occurs at the sorbent molecular level, and it alters the composition and morphological structure of a solid sorbent. Therefore, during the process, a material expansion typically occurs and significantly higher activation energy than for adsorption is present. This energy is mainly related to covalent bonding of atoms and molecules. Absorbents can be liquids or solids, and the main difference is that their concentration during the reaction process varies stepwise for solids or continuously for liquids. Absorbates can be liquids or gases, which have a different amount of binding energy released as heat of reaction. If the absorbate is in liquid state, part of the binding energy is needed to break the bonds within the liquid, therefore, only part of it will be released as heat of reaction. For absorbents in vapor state, all the binding energy is released as heat of reaction.

Adsorption is defined as the phenomenon occurring at the interface between two phases, in which cohesive forces act between the molecules of all substances irrespective of their state of aggregation. Therefore, adsorption occurs at the surface of the adsorbent forming an extremely thin layer of atoms or molecules on the adsorbent surface, while leaving its structure unaltered. No expansion occurs and no or negligible activation energy is involved. The sorption energy is typically related to the weak intermolecular forces (Van der Waals forces) and hydrogen bonding and no activation energy is required (6).

The adsorption property of surfaces were discussed by Langmuir firstly and then by Brunauer–Emmett–Teller which formulated the BET theory (7). Langmuir assumes that only one layer of adsorbed material can exist on the sorbent surface, while according to the BET theory an infinite number of layers can be formed. Following this principle, 5 distinct types of isotherms can be plotted depending on the morphology of the porous structure (Fig. 2.2).

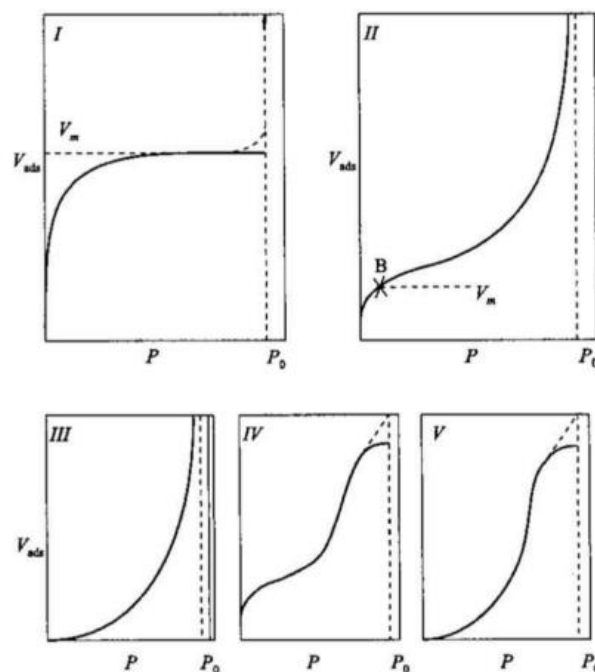


Figure 2.2 – 5 type of isotherms (BET theory) based on the morphology of the solid

Curve I represents the Langimur theory of single layer coverage, can be attributed to physisorption by microporous adsorbents with relatively small external surfaces. Curves II, III, IV and V are typical for multi-layer adsorption. In particular isotherm of type II are normally obtained with non-porous or macroporous adsorbents, type IV is characterized by adsorbents which possess mesopore structures, such as many silica gels and other porous oxides, while curves III and IV indicate weak gas-solid interactions (8).

Compared with SHS and LHS technologies, Sorption heat storage has the highest theoretical energy density among the three categories of heat storage, arising from the large bonding force between the sorbent and sorbate, and the heat losses can be, in principle, negligible, due to the fact that sorbent and sorbate can be kept separated. This, in turn, can result in a more compact system, which makes this technology prone to be used to store large quantities of energy over a relatively long period (9).

The relevance of storage systems based on sorption phenomena thus lies in their high energy density and their negligible heat loss and the repetitiveness of storage operations. It is possible to see from the Fig. 2.3 that materials used in sorption storage have the highest storage density of all repetitive storage media in the range of low operating temperature (90-150 C° is the range in which the solar panel work). With the aforementioned characteristics of sorption materials, it is possible to consider long-term solar energy storage, in particular seasonal storage, based on sorption, a process that gained recently a renewal of interest in research platforms, even if currently we are not at a sufficient level of maturity that permits the complete commercialization of this technology (10).

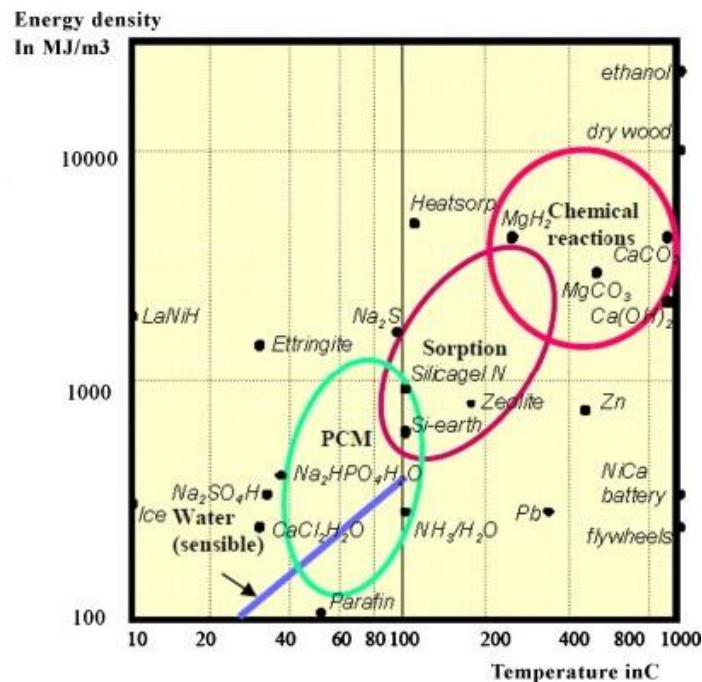


Figure 2.3 - Energy densities for the different TES mechanisms, among which the STES has the highest energy density, followed by the latent heat storage system. With a high energy density, the volume required to store the energy should be reduced

Storage materials represent the basis in the development of a STES system. The state of art of this kind of technology is still under researches and is continuously improving, therefore the aim of this work is to provide an overview on the most recent researches and development of the technologies in the field of sorption thermal energy storage, with particular attention on the materials adopted for sorbents and sorbates.

## 2.4 materials for sorption heat storage

The following part is dedicated to the explanation of the main working principles of each category of sorbents while a comparison between their performances is proposed at the end of the chapter.

Sorption materials are the basis for developing sorption energy storage systems. There are a great number of materials that could be used for sorption when focusing only on the thermodynamic principle of reversible reactions. Some technical, economic or ecological criteria lead to a closer set. Usual selection criteria of materials are:

- high affinity for the sorbent by the sorbate: this has an effect on the rate of the ab/adsorption reaction, which is important for an usable power density
- high sorption capacity: influenced by sorption temperature and pressure, estimated using sorption isotherms and isobars
- high storage density, that influences also the volume occupied by the material sorbent. One of the main purpose in the latest researches in the field of sorption materials is to identify the one with higher density and so with the lower volume in order to guarantee at the storage system the effectiveness by employing as little material as possible.
- Large thermal conductivity and good heat and mass transfer, in particular from the sorbate to the heat exchanger. A higher thermal conductivity could decrease the sorption temperature during the discharging process and thus enhance the sorption rate and sorption capacity
- Low charging temperature, this results in high solar collector efficiency
- Non-toxicity, non-corrosiveness, and non-harmfulness to the environment and humans

Depending on the interface between adsorbent and adsorbate, adsorption can be divided into four types: solid/gas, solid/liquid, liquid/liquid, liquid/gas. The solid/gas adsorption has been widely used and studied, playing a pivotal role in interface chemistry (11).

### 2.4.1 liquid absorption

Systems based on liquid absorption rely on the mechanism of absorption of a fluid (solvent) inside a liquid (solute) and imply the change of concentration of these substances during the cycle.

The most common couple are  $LiBr/H_2O$  and  $H_2O/NH_3$ , both working solar cooling applications, due to good performance of these liquids at the temperatures available from conventional collectors.

Berlitz et al. (11) proposed three different storage mechanisms to exploit the  $LiBr/H_2O$  couple: external storage by means of thermal oil, external storage with sensible heat of cold water and an internal storage with latent heat of the refrigerant water and  $LiBr$  solution. The result was that the internal storage was the best configuration that led to a cooling capacity of 20 kW and a need for cold storage of 3.3 kWh.

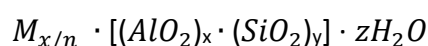
The drawback of this kind of storage are safety parameters, since risk of flammability, reactivity or toxicity and high investment cost.

## 2.4.2 solid adsorption

Physical adsorption (physisorption) is a general phenomenon whenever an adsorbate is brought into contact with the surface of the adsorbent, in which cohesive forces, including Van der Waals forces and hydrogen bonding, act between the molecules of all substances. The performance of adsorbents used in physisorption is governed largely by surface properties, such as surface area, micro-pores and macro-pores, size of granules in powders, crystals or in pellets. Thus higher the surface of the adsorbent, higher the quantity of sorbate that can be adsorbed, higher the quantity of energy that can be stored. Moreover other features requested to solid adsorbents are good mass and water transport, in fact, high porosity and high specific surface area allow superior and faster water adsorption. Adsorbents having special affinity with polar substances like water are termed 'hydrophilic'. These include silica gel, zeolites and porous or active alumina. Non-polar adsorbents, termed 'hydrophobic', have more affinity for oils and gases than for water. These substances include activated carbons, polymer adsorbents and silicalites (12).

Silica gel is a high porous, non-crystalline form of silica ( $SiO_2 \cdot xH_2O$ ), with excellent capacities for adsorption of water (up to 30-40% of its dry mass), making it suitable for use in low temperature sorption systems. If it is overheated and loses this water, its adsorption capacity is lost and therefore it is generally used in temperature applications under 200°C (13). In a series of recent studies by AEE-INTEC (Institute for Sustainable Technologies, Austria) (10), in which silica gel was adopted for SSHS (closed systems), a material storage density of about  $50 \text{ kWh/m}^3$  was achieved experimentally, even if it is estimated that the energy density by a physisorption of other material can reach the value of 200-300 kWh/m<sup>3</sup>, showing that it is less efficient with respect other solid material and rejecting the idea of silica-gel exploited in long and also short-term storage applications.

Zeolites consist of porous crystalline aluminosilicates of alkali or alkali earth elements such as sodium, potassium and calcium. The general formula of zeolite is:



with x and y integers with their ratio larger than one; n the valence of cation M, and z the number of water molecules in each unit cell (6).

Zeolite is a good candidate to be used in reactor studies because of its high stability and its ability of large energy sorption density and capacity, due to the higher strength of sorbent-sorbate bond

which characterize its mechanism of adsorption. In addition the regular porous structure allows good mass and heat transport, making this a good fit as a hosting matrix material for other sorbents.

Several aggregates of zeolites can be produced, Type 13X is reported as one of the best performing zeolites for heat storage purposes due to a high water uptake and fast reaction kinetics. This idea has been proved by a research conducted by Hauer (10), who, using the synthetic Zeolite 13X, reached experimental storage density of  $124 \text{ kWh/m}^3$  for heating and  $100 \text{ kWh/m}^3$  for cooling.

However, besides the optimal level of energy density that can be reached, storage systems using zeolites as sorbent material or as hosting matrix are very expensive due to the high production costs (in the range of 1-3 €/kg), making the adoption in the commercial use of this material very scarce.

Some new classes of materials, including aluminophosphates (AIPOs), silico-aluminophosphates (SAPOs) and metal-organic frameworks (MOFs), have recently emerged as promising porous materials for heat storage. AIPOs refer to a class of microporous, crystalline aluminophosphate phase recently discovered similar to zeolite in the field of adsorption properties (14).

Analyzing in detail some of these compounds, i.e. AIPO-18 and SAPO-34 samples, it can be state that they have the best performances considering the most favorable operating conditions of thermal heat storage, which are a low charging temperature and adsorption water vapor pressure similar to the saturation water vapor pressure at ambient temperature. In particular, for low temperature heat storage purposes, SAPO-34 and AIPO-18, two of the most widespread and efficient materials of this class, are found to have remarkable energy densities (203 and 243 Wh/kg respectively) with a charging temperature of  $95 \text{ C}^\circ$  (6).

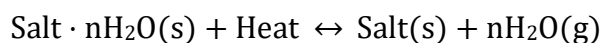
MOF is a relatively novel class of porous materials gained attention in the past years due to its high sorbate uptake potential, that can arrive at  $1.6 \text{ GJ/m}^3$  of energy density with a low desorption temperature ( $90\text{-}140 \text{ C}^\circ$ ). Even for both these new classes of material the price is extremely high so as they cannot be taken in consideration if the aim is to research a cheap material.

### 2.4.3 solid absorption

The interest in the solid absorption process (chemisorptions) mainly focus on the possibility to create strong bond between the absorbate and the absorbent (chemical bonds), consequently having the advantage to absorb a biggest amount of  $H_2O$  and to store more energy.

Extensive research on salt hydrates is being carried out for chemical reaction in thermal storage applications. The main reasons are a high theoretical energy density of the materials, desorption temperatures achievable with solar thermal collectors, and discharge temperatures useful for lowtemperature heat applications such as space heating and domestic hot water production.

The general reversible reaction of a salt hydrate can be written as follows:



being  $n$  the number of water moles involved in the reaction and “Heat” the thermal energy exchanged [kJ/mol].

The main drawback of the hydration of hygroscopic salts is the phenomenon of the deliquescence: in some cases the relative humidity/pressure is so high that the product of the hydration is a saturated salt solution, rather than a salt hydrate. Deliquescence is defined as a first order phase transformation from the solid state to a saturated solution when the relative humidity (RH) reaches a certain threshold value, namely, the deliquescence relative humidity (DRH), property of the salt and the temperature (11). At a macroscopic level the deliquescence manifests itself with a tiny liquid film on the surface of the hygroscopic salt that could prevent from hydration and could cause problems of corrosion. The consequence is the leakage of the chemical material in the liquid state which cannot be recovered for storage applications.

The most important parameters that a salt should meet for thermochemical energy storage to be implemented are high energy density, high permeability and high heat conductivity. Other aspects to be considered do not depend on the material storage capacity, such as the type of system considered (open or closed).  $\text{NH}_3$ -salt, even if it presents a high storage density, is an example of a working couple that cannot be employed in an open system, since it is a dangerous material to be dispersed in the environment during the mass-exchange moment.

The salt with the highest theoretical volumetric energy density shown here is  $\text{Na}_2\text{S}$  in the anhydrous form, that can reach an energy density of 3.17 GJ/m<sup>3</sup>, but this salt presents the disadvantage of formation of toxic  $\text{H}_2\text{S}$  gas during hydration (15).  $\text{MgCl}_2$  has a volumetric energy density almost as high as  $\text{Na}_2\text{S}$ , but the disadvantage of the slow hydration and dehydration rate. The cheapest salt hydrate with a reasonable energy density is  $\text{Na}_2\text{SO}_4$  that can reach an energy density of 2.56 GJ/m<sup>3</sup>.  $\text{MgSO}_4$  is also relatively cheap with a reasonable volumetric theoretical energy density of 2.81 GJ/m<sup>3</sup>, and a high DRH (90% at 30°C) (11), but with the drawback that it has a melting temperature lower than the dehydration one, with the risk of melting, even if this can be avoided adopting small particles of salt (16).

When dealing with salts it is fundamental to consider the melting and deliquescence points, or the corrosive properties that characterize many salts. If these aspects may lead to consider salts as the worst candidates in sorption storage applications, on the other hand utilization of pure salt impregnated in host matrix may enhance heat transfer and energy storage, as it is explained in paragraph 2.4.3.

## 2.4.4 composite materials for sorption heat storage

As presented in the previous chapter, scientific research in recent years has moved towards an optimization of STES systems, taking into account the advantage to have abundance of hygroscopic salts to be exploited as sorbents, characterized by high energy density. However,

though chemical reactions possess excellent storage potential based on the analysis on the material level, some drawbacks must be considered, as the phenomena of deliquescence of salts, a phase transformation whereby a substance absorbs water vapor from the atmosphere, leading to the dissolution of the solid and the presence of bulk water in the system at partial vapor pressures less than 1 (17), that leads to a low cyclability. On the other side, solid microporous sorbents such as zeolites or silica gels, are characterized by a high level of hydrothermal stability, with higher power outputs and cyclability, at the expenses of lower energy densities and higher cost.

The most promising theory to overcome the issues related to the aforementioned sorbents is to exploit some composite sorption materials which are formed by at least two components. The one serving as the host matrix, while the other working as the active sorption material (the salt hydrate). The above composite materials are also referred to as 'salt inside porous matrix' materials (CSPM). The host matrix is important in order to prevent salt agglomeration, and swelling, which leads to an improvement in moisture diffusion during heat regeneration. Clearly, the host matrix must be highly porous, so as to host a considerable amount of salt crystals. In case of hydrophilic sorbents (such as zeolites or silica gels) used as host matrices, they can give a contribution to the sorption heat released by the composite (18). The main advantage of the CSPM composite is the possibility to rely on both active and passive material, respectively the salt and the matrix, to increase the thermal energy developed by the hydration and dehydration phenomena, and moreover to tune the percentage of the different sorbents operating on this process to obtain different configurations.

During the discharge phase (adsorption) water is adsorbed in the micro-pores of the structure (physisorption), the anhydrous salt chemical reacts with water (chemisorptions) and crystalline hydrates are produced and confined inside porous matrix. Next, deliquescence and dissolution of salt hydrates occurs until the host matrix is filled with salt solution (19). While the saturated salt solution gradually becomes a dilute salt solution, absorption process continues until equilibrium point. The desorption phase (charging) starts when thermal energy is provided to the composite, crystallization of the saturated salt solution and efflorescence of crystals occur and heat is stored in the separated salt and water adsorbed inside the micro pores in the form of absorption, chemisorption and physisorption potentials successively.

In the literature there are many experiments aimed at finding the most performing combination of CSPM material in a temperature range of 30-150°C.

Casey et al. (2) tested salt composite with matrices of vermiculite, zeolite 13X and silica gel. The salt adopted were  $MgSO_4$ ,  $LiBr$ ,  $CaCl_2$ ,  $Li(NO_3)_2$ . Pure matrices follow a type I isotherm based on Langimur theory, whereas, in the case of impregnation with salt, the obtained curve is one of type IV, which indicate an higher level of adsorption uptake. The best performance in terms of energy density are obtained with two composites with a matrix of vermiculite impregnated with  $CaCl_2$  or  $LiBr$ , which reach respectively values of 0.179 and 0.167  $GJ/m^3$ , even if it is considered a poor result since a water storage with a temperature step of 50°C can store approximately 0.2  $GJ/m^3$  (6).

Hongois et al. (11) prepared a zeolite/*MgSO*<sub>4</sub> composite (ZM15) for low temperature heat storage applications reaching energy density of 166 kWh/m<sup>3</sup>, with a percentage of the salt inside the composite of about 15%. The *CaCl*<sub>2</sub>-silica gel composite for thermal energy storage has been extensively studied by Wu et al. and Zhu et al. (20). The composite sorbent prepared by impregnating of silica gel with a 30 wt.% *CaCl*<sub>2</sub> solution exhibited a storage capacity of 283 Wh/kg at the relatively low charging temperature of about 90 °C.

In conclusion, as it is summarized in Fig.2.4 that provides an overview of the energy density reached by the different sorbents in relation with the charging temperature, chemisorption sorbents appear to have the greatest energy density achievable. However, the presence of aforementioned drawbacks of deliquescence, inapplicability in open systems since sorbate and sorbent cannot be kept separated from environment, make them an inappropriate material to be used in STES applications.

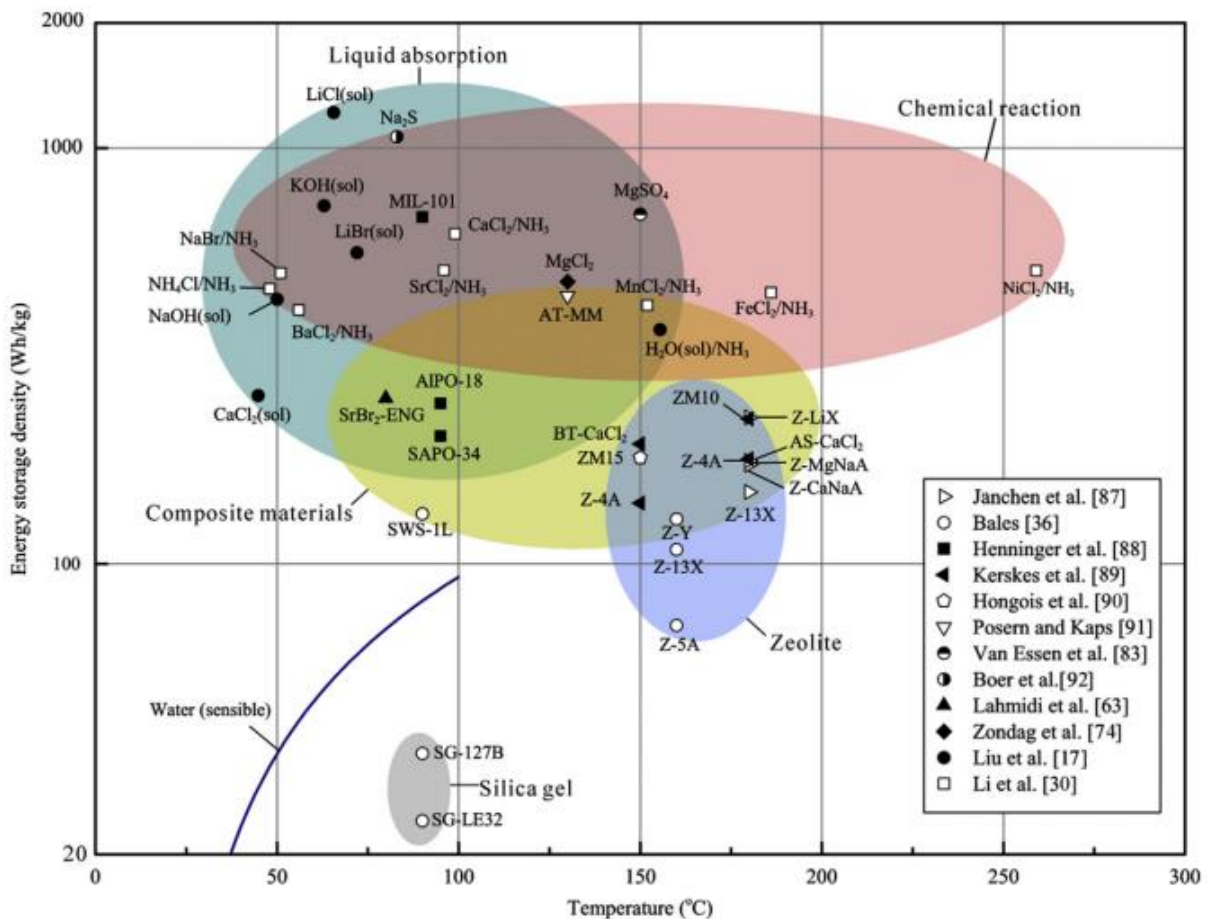


Figure 2.4 - Energy storage densities of sorption materials

Even liquid sorption emerges as a good candidate in terms of energy stored since its high energy density, but it loses its attractiveness looking at Fig. 2.5 (21), that represents the storage capacity cost (SCC) with respect the charging temperature. SCC is a key parameter to compare sorbents material among themselves considering their commercial price. It is defined as:

$$SCC = \frac{\text{euro/ton}}{ESC \cdot 1000} \cdot 3.6$$

and generally is expressed in €/kWh.

It is evident the high SCC in liquid materials that added to the risk of flammability or reactivity make them not convenient for a STES application.

Same consideration can be done for solid sorbent: on one hand AIPOs, MOFs and zeolites have the best performance in terms or sorption properties but very high cost, on the other hand silica gel is cheaper than the others but presents low values of energy stored.

In this scenario composite material appears to be the most promising sorbent to be employed in STES application, capable of providing an adequate compromise in terms storage capacity, compatibility with thermal storage systems, availability, cyclability and price.

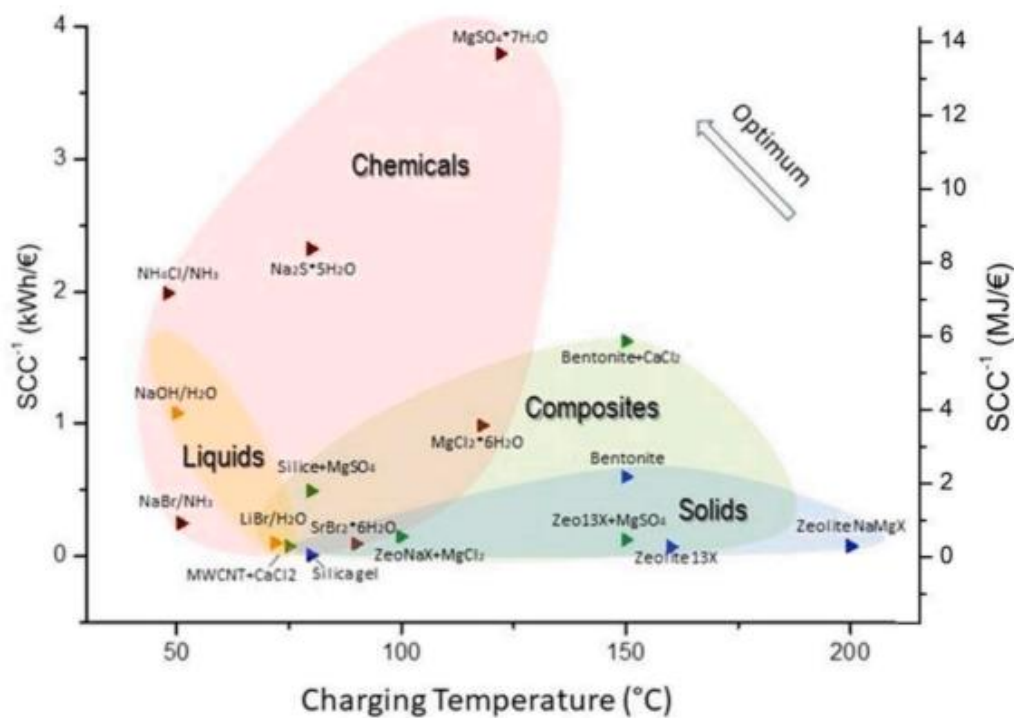


Figure 2.5 - storage capacity cost in relation to charging temperatures for the sorbent materials (21)

In recent times, with the aim of maximizing energy density and minimizing costs, several researches started to consider cement as one of the most promising candidate as matrix to accommodate salts in composite materials.

## 2.4.5 cementitious composite materials

The concept of cement-based composite materials is directly obtained by mixing the cement paste with salt hydrates, thus exploiting the natural porosity formation in cement and a salt crystal precipitation within the pores. Below, this new approach will be referred to as in situ synthesis.

The possibility to adjust the porosity of the cement by controlling the quantity of water in the mixing makes this material attractive for sorption thermal storage purpose. In addition the fact that it is widely spread in nature, easy to handle and cheap makes it very interesting for research operations. As an example, for pure cement powder, it is assumed a price ranging from a maximum of 155 €/ton and a minimum of 80 €/ton, according to a EU report on the competitiveness of the European cement sector. On the other hand, considering a common Zeolite 13X, the price assumed is about 2500 €/ton.

In the past preliminary analysis on the properties of the new cement-base composite material (18), focusing predominantly on Energy Storage Density (ESD, MJ/m<sup>3</sup>), Energy Storage Capacity (ESC, kJ/kg), Storage Capacity Cost (SCC, €/kWh),  $MgSO_4$  was introduced into the porous matrix and a calorimetric experiment was carried out in order to characterize the thermal performance of the composite. The latter allowed to reach an Energy Storage Density of 0.28 GJ/m<sup>3</sup>, and on the base of a cost analysis, useful to compare sorbent materials for TES applications, an energy of 0.3 kWh/€ is obtained. It overcomes that of porous Zeolite 13X, one of the most interesting materials for water sorption heat storage, but with the huge drawback of being very expensive.

The aim of this thesis is to continue to investigate cement-base composite materials starting from this previous consolidate research and proceeding towards other salt hydrates tests, bearing in mind the objective to obtain the composite with the higher energy density and the lower expense. The main criteria for the selection of materials and the parameters through which materials are evaluated are: volumetric energy storage (it could be intended as ESC or ESD), thermal and chemical stability, low cost and high availability, low charging temperature.

## 2.5 storage systems

Moving towards system based upon TCM materials allows to exploit their main features as the high energy density and the possibility to build long-term storage plants, known also as seasonal storage plants, since the heat from the summer can be stored and provided in the winter season. The latest researches aim to test the best materials in order to design the most efficient low-temperature long-term sorption heat storage system. Thus the materials, in addition to being the

most efficient from the thermodynamic point of view, must above all meet the criterion of being suitable at a system-scale. Depending on the system configuration that is chosen to implement TCM for building applications, the equipment is composed of the reactor, heat exchangers, vessels, evaporator/condenser, solar collectors, valves and piping. The main difference in the classification of sorption systems is between open and closed solid sorption systems, both based on their working principles.

The main features of open systems (Fig.2.6) is that mass and energy are exchanged with the environment, typically at environment pressure. The moist air is captured from the surrounding and plays the role of both sorbate material and heat transfer fluid (HTF). An humidifier is needed to increase the of the inlet air. During the charging process, the inlet air is heated to obtain hot dry air, which flows through the saturated sorbent placed in the reactor, to release the sorbed water.

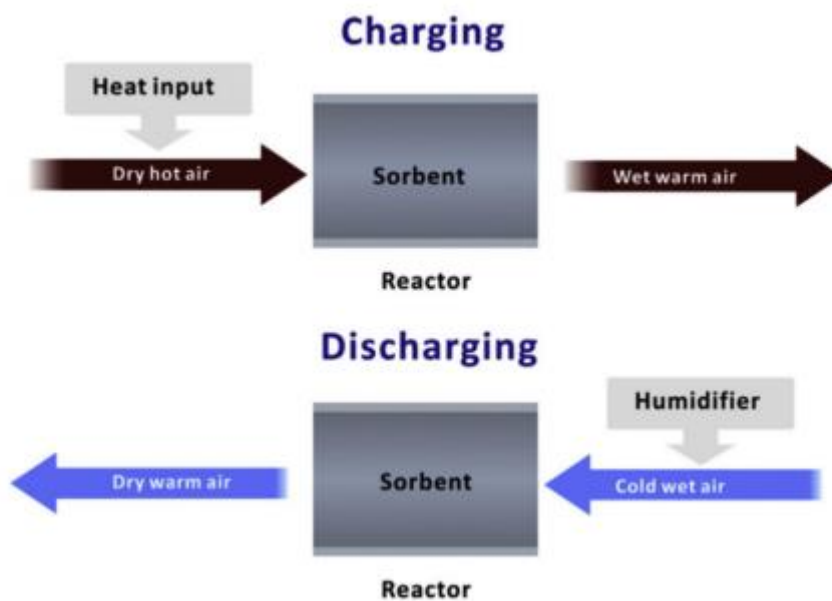


Figure 2.6 - schematic representation of an open thermal systems

In the discharging process, moist air flows through the unsaturated sorbent, while the inside moisture is sorbed, and the sorption heat is released to the surrounding air. The main advantage is that the system is generally simple, not expensive, not pressurized, it has a good and controllable heat transfer and requires less components compared to a closed one. The main disadvantages of these systems are that a fan is needed to drive the moist flow through the reactor, a humidifier can be required to reach the desired sorbate vapor pressure, and the temperature step over the reactor is limited by the thermal mass of the flow, which requires a heat recovery unit to obtain temperatures useful for space heating and domestic hot water production. Moreover, due to the fact that mass is also exchanged with the environment, dangerous materials and components cannot be employed (22).

On the other hand closed systems (Fig.2.7) exchange only energy with the environment, sorbate and sorbent are isolated from the surrounding. Such systems basically comprise a reactor packed with the sorbent put in contact with an heat exchanger and an evaporator/condenser that supplies or recovers the sorbate. The role of the condenser is avoiding to store water in a vapour state because it would require a high volume, for this reason it is condensed and when water is needed it is returned in the gas state by the evaporator. In the charging process, the saturated sorbent inside the reactor is regenerated by the hot HTF heated by a charging heat source. The sorbed sorbate is released in the gaseous state and flows into the evaporator/ condenser, where it condenses into a liquid under the condensation temperature, and the condensation heat transfers to the heat sink. In the discharging process, the unsaturated sorbent inside the reactor sorbs the gaseous sorbate, which flows from the evaporator/condenser at a constant temperature, and sorption heat is released to heat the HTF for heating applications. The main system advantages are that a fan is usually not needed since the sorbate is driven by the vapor pressure difference between the system components, a faster transport mechanism compared to diffusion in open systems and it is possible to use materials that could be toxic in an open system because they are dispersed in the environment (for example the ammonia  $NH_3$ ). The drawbacks are the wide volume occupied by this type of plant, due to the presence of the evaporation/condenser configuration and consequently the difficulties that arise in the design and manufacturing of the different components and the increased cost.

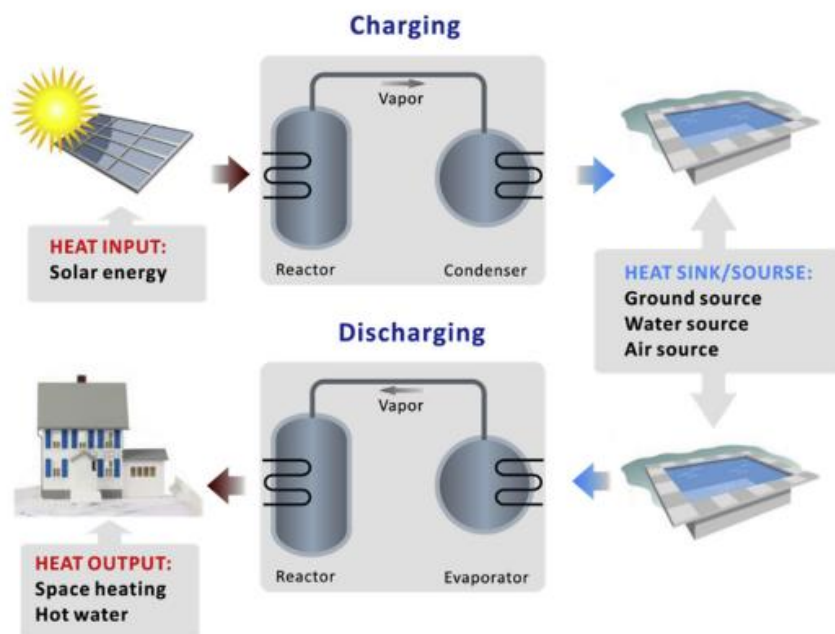


Figure 2.7 - schematic representation of closed thermal systems

## 2.6 thermodynamic cycle

The working cycle for an adsorption TES can be represented on the Clapeyron diagram, in which the x-axis and y-axis represent respectively the logarithmic scale of the temperature and the logarithmic scale of the pressure (Fig 2.8). The red lines represent the charging phase (desorption) while the blue lines the discharging phase (adsorption). During charging phase (i.e. desorption), heat is introduced in the system ( $Q_{des}$ ) and it is exploited to regenerate the sorbent material which is saturated of adsorbate. This amount of energy can be distinguished, following the cycle in Fig, in two different quantities:  $Q_1$ , usually known as isosteric heat, which represents the amount of sensible thermal energy spent to heat up the adsorbent material and the adsorbate under isosteric conditions, during which no desorption happens (1-2 segment of the cycle). The actual desorption phase takes place following the segment 2-3, where  $Q_2$  is the energy spent to desorb the adsorbate from the material accompanied by the increase of temperature up to the final temperature,  $T_{max}$ , in the adsorbent material. The heat of condensation,  $Q_c$ , is usually dissipated in the ambient or nevertheless, if needed, it can be also exploited by the user in daily heat storage applications, for instance by storing it in a buffer heat storage. Once the charging process is completed, thermal energy can be stored as adsorption potential, condenser and reactor are kept separated and heat is preserved. During this discharging phase (i.e. adsorption), the adsorbate is evaporated adsorbing heat from the ambient,  $Q_{ev}$ , then the vapour fluxes to the adsorber, since the adsorption process is exothermic, heat is released to the user,  $Q_{ads}$ . Also in this case,  $Q_{ads}$  comprises two different components,  $Q_3$  which represents the energy delivered during isosteric cooling down process, which brings the pressure down to the evaporator pressure (segment 3-4) and  $Q_4$  which mainly represents the energy associated to the enthalpy of adsorption (segment 4-1) (23). The process can be defined “closed” since the sorbate follows continuously evaporation-condensation cycles, without mass or heat transfer with the environment.

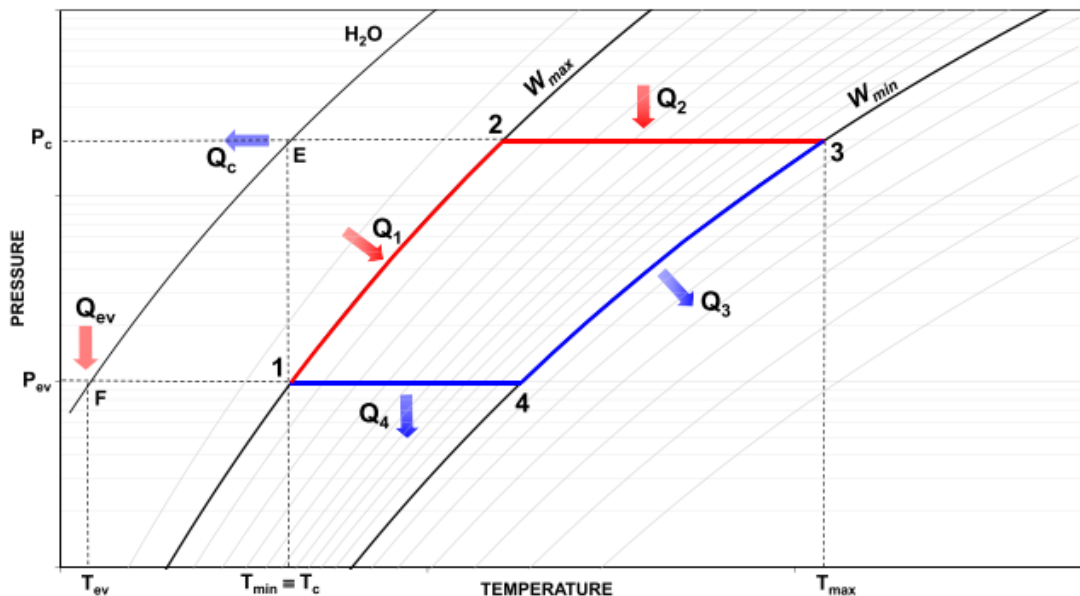


Fig 2.8 - Working cycle of an adsorption heat storage

# 3.Cement: fundamentals and main features

As mentioned above, cement is the researched material that constitute the matrix of the composite material for the STES applications. The choice fell on this substance for the great availability and the relatively lower cost with respect all the other matrix material that until this moment were adopted such as zeolites, serotypes, silica gel. In this chapter the principal characteristic of the cement will be analyzed in order to understand the reason that led to the adoption of this material for STES applications.

Cement generally refers to a very fine powdery substance chiefly made up of limestone (calcium), sand or clay (silicon), bauxite (aluminum) and iron. It is one of the most important building materials, is a binding agent that sets and hardens to adhere to building units such as stones, bricks, tiles, etc. In addition it is used to make concrete as well as mortar, and to secure the infrastructure by binding the building blocks. Cement mixed with water causes a chemical reaction (hydration) and forms a paste that sets and hardens to bind individual structures of building materials (24).

Portland cement is the most widespread cement based materials in the world, it is estimated that it fills the 97% of the whole world market of the cement (25). Portland cement is generally the basic constituent to make concrete because is suitable for wet climates and can be used under water.

## 3.1 cement production

Portland cement was first produced by a British stone mason, Joseph Aspdin in 1824, who cooked in his kitchen a mixture of limestone and clay powder, then he grinded the compound until he created the cement powder that hardens when it reacts with water

The stages of the modern manufacture procedures of Portland cement (Fig 3.1) are:

- Mixing of raw material
- Burning
- Grinding
- Storage and packaging

The major raw materials used in the manufacture of cement are Calcium (especially limestone), Silicon (clay powder, sand), Iron and Aluminum. The mixing phase is performed in two processes: dry and wet process.

During the dry process the aforementioned materials are grinded in the gyratory crushers to get 2-5cm size pieces separately. Once fine particles are obtained, each material is provided in the adequate proportion and is mixed so that the average composition of the material is maintained.

In the wet process, raw materials are pre-crushed and then mixed with water in a washmill, maintaining the correct proportion in the mixture, obtaining a paste called slurry, that contain around 40% of water.

In both cases, the mixture produced is stored in silos (a raw mix in the dry process and the slurry material in the wet process) and kept ready for the burning process. A brief comparison between the two mixing methods underlines that the case of wet process is cheaper and produces a mixture of higher quality, even if the time of process is higher due to the adding of water and the mixing with it.

The burning process takes place in the rotary kiln, a steel tube inclined with the inner side lined with refractory bricks. The raw mix of dry process or the slurry of wet process is injected into the kiln from the upper end, while the kiln is heated from the lower end. A slow rotation movement of the inclined kiln helps the raw material to fall towards the lower part that is heated. In the upper part, water or moisture in the material is evaporated at 400°C, so this process is known as Drying Zone. In the lower part (clinkering zone) the temperature is in the range 1500-1700 °C and in this zone the lime and clay of the cement react and produce aluminates and silicates. These products of the chemical reaction fuse and form small and hard stones known as clinker. The size of the small and hard clinkers varies from 5 to 10mm. Then the clinker is cooled by air and exits the kiln from the base.

The cooled clinkers are sent into mills, where they are ground finely into powder. Powdered gypsum is added around 5% as a retarding agent during final grinding in order to do not allow the cement to settle quickly when it comes in contact with water.

In the final stage the ground cement is stored in silos, from which it is marketed either in container load or 50 kg bags.

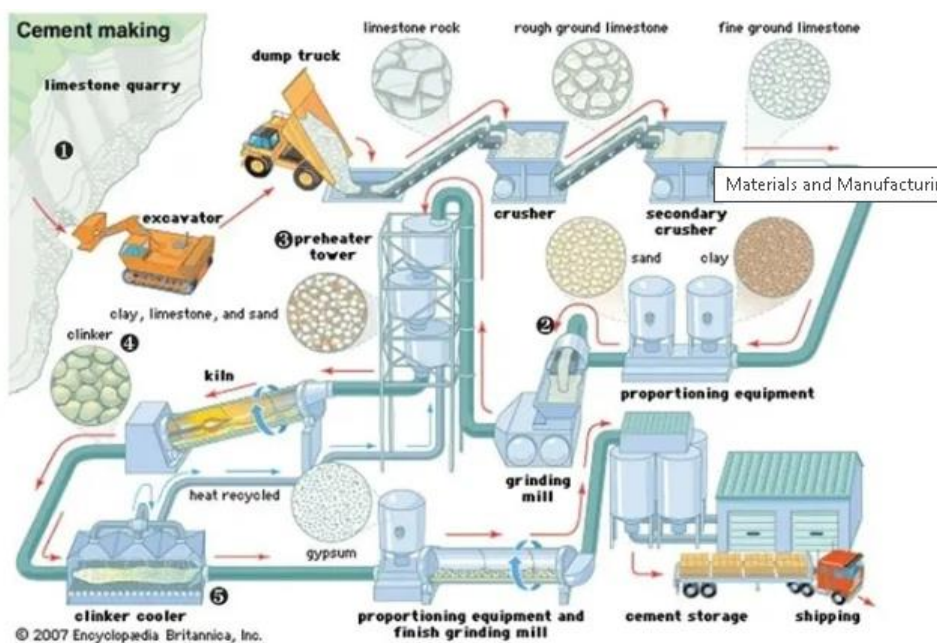


Fig. 3.1 - graphic scheme of the cement production

## 3.2 cement composition

Portland cement is made up of four main compounds: tricalcium silicate ( $3CaO \cdot SiO_2$ ), dicalcium silicate ( $2CaO \cdot SiO_2$ ), tricalcium aluminate ( $3CaO \cdot Al_2O_3$ ), and a tetra-calcium aluminoferrite ( $4CaO \cdot Al_2O_3Fe_2O_3$ ). In an abbreviated notation differing from the normal atomic symbols, these compounds are designated as  $C_3S$ ,  $C_2S$  (called silicates),  $C_3A$ , and  $C_4AF$  (also called aluminates), where C stands for calcium oxide (lime), S for silica, A for alumina, and F for iron oxide. Aluminates constitute the larger part in the whole composition of the cement, moreover these compounds show the tendency to set very fast when the cement is hydrated. In order to slightly improve the malleability of the cement past, an amount of about 5% of gypsum ( $CaSO_4 \cdot 2H_2O$ ) is added to the clinker during the production and it has the role to retard the setting phase.

When cement powder is mixed with water starts the hydration process, that includes a number of exothermic chemical reactions that take place in different times. First start the adsorption of the molecule of water on the surfaces of the dry powder and the dissolution of some compounds occur. The more reactive compounds with water are the aluminates and the velocity rate of hydration is influenced by many factors as w/c ratio, specific surface area of compounds, temperature. They are responsible for the setting time of the cement, indeed water induces the diffusion of ions  $SO_4^{2-}$  and  $Ca^{2+}$  from the aluminate  $C_3A$  and thus producing ettringite, a trisulphate compound which slows the hydration process because it covers the cement molecule and avoid contact with water. For this purpose the adding of the gypsum is important: it produce a continuous coating on the surface of  $C_3A$  that impedes diffusion of ions and retard the setting phase.

On the other hand the hydration of silicates is slower with respect aluminates. This time coincides with the production of a family of amorphous calcium silicate identified as C-S-H or C-S-H gel, because the consistency is similar to an amorphous gel with a variable stoichiometry. This gel is responsible for the hardening and strengthening of the cement: it is In this phase that cement viscosity increases and the solidification advances (26).

## 3.3 porosity

Three main types of porosity can be mentioned speaking about cement:

- Gel porosity
- Air voids
- Capillary porosity

During the hydration process the calcium silicate product C-S-H appears as an amorphous phase with a variable composition in which many gaps are present, precisely the gel porosity, but the dimensions are so small (a few nanometers) that do not affect the mechanical properties of the cement.

Air voids are due to some air that remain stuck in the solidified cement, they have spherical shape and dimension in the range of 100-300  $\mu\text{m}$ .

Capillary porosity arises from the fact that after the hydration process, the water that reacted with dry powder cement leaves place to the product of the hydration, but not all the quantity of water participates at the reaction, so if there is some amount in excess it remains stock between the reaction products, so it evaporates and some voids remain in the solidified cement. The reaction between cement and water follows a stochiometric law, so considering the w/c ratio, where w is a well defined mass of water and c a well defined mass of cement, if w/c ratio is 0,42 it means that all the water reacted with all the cement and the hydration process is complete, so there is no present of water in excess and capillary porosity cannot form. With the increasing of the amount of water it can be seen an increase in the quantity of capillary porosity.

Since one of the main parameters in the choice of the material matrix for the composite element capable of store the greater amount of heat is to be porous, in order to accommodate a big quantity of hygroscopic salts, so the parameter w/c is one of those on which we have focused more to test the different samples of cement.

### 3.4 bleeding

Bleeding is a phenomenon that occurs in concrete and it manifest itself as a layer of unmixed water that rises up on the surface of the cement past. The cause of this phenomenon is the segregation, for which the heavy aggregate particles settles down while water rises up to the surface and forms a layer. Due to bleeding the quantity of water supposed to mix with powder cement decreases, so it leaves voids inside the cement and this increases the porosity. Moreover the theoretical w/c ratio will be higher than the actual w/c ratio because at the end of the process there will be an amount of unreacted water that remains in the surface. Process of bleeding is a normal phenomena if it is at normal rate but can create weakening of bond if occurs at high rate. One of the advantage of bleeding is that it replaces the water lost by evaporation and prevents the surface from drying quickly before it has attained sufficient strength to resist cracking. The effect increases with the increasing in the w/c ratio, so when it is necessary to work with high w/c ratio in order to obtain high porosity in the cement past, some anti-setting agents are added in the misture (bentonite is an example of anti-setting agent). Other methods to reduce bleeding are using finer cement powder, because smaller particle hydrate faster and so the rate of water expulsion is lower, or using air entraining admixtures (27).

## 4. Materials and Procedures

This chapter describes the experimental part carried out for the thesis, in order to achieve the aim to find a proper composite material to employ in STES application. The treatments and the technical steps executed in the laboratory are here presented including the measurements and the calculations developed.

The materials employed are the Portland cement, mixed with de-ionized water to create the samples and the hygroscopic salts are  $CaCl_2$  (Calcium Chloride) and  $MgSO_4$  (Magnesium Sulfate). In this specific research the cement Portland cement is provided by the Italian company Italcementi and is called ULTRACEM 52,5 R, while the salts are distributed by the company Merck. Magnesium Sulfate was chosen in his epta-hydrated form  $MgSO_4 \cdot 7H_2O$ , since it is one of the most promising hygroscopic salt for compact seasonal heat storage. It can be dehydrated at temperature below 150 °C, working temperature of the solar collector, and then hydrated with water vapor pressure at 1,3 kPa in order to release the heat stored (16).

The steps of the research include the preparation of samples of pure cement mixing water and dry powder, then accurate measurements allow to calculate density and porosity, the two main parameters needed to evaluate the quantity of salts to introduce in the matrix. To reach this aim two techniques are applied: dry impregnation and a new procedure called in-situ synthesis (18). Once samples of composite materials are obtained and the densities and porosities are estimated, a first thermal analysis in the laboratories of the Department of Applied Science and Technology (DISAT at politecnico di Torino) is carried out. It is needed to evaluate the more promising sample from the point of view of thermal heat generated when they come in contact with the liquid sorbate. Then, a more specific adsorption analysis was carried out at the Italian National Institute for Metrological Research (INRiM) to estimate the thermal properties needed to define the proper material.

### 4.1 matrix preparation

The matrix of the composite material under consideration is made up of cement, so the sample prepared are composed by mixing dry powder of Portland cement with de-ionized water. The parameter to take into consideration is the w/c ratio, mass of the water divided by mass of the cement powder. The stoichiometric ratio that allows the complete hydration of cement is 0.42, but since it is essential to have a porous matrix the samples are manufactured with elevated ratio, specifically ratio of 1, 1.5 and 2. A little quantity of anti-settling material is added during the mixing, specifically about 1% with respect to the mass of dry powder considered. The purpose in adding this component is to counter the effect of bleeding, phenomenon due to the high w/c ratio considered for the samples as exposed in the paragraph (paragraph 3.3). The mixture of the precise quantity of water and cement takes place in a beaker with the rotation of a mechanical stirrer until semi-viscous slurry is produced and then poured into proper metallic molds. This is composed by four rectangular cavity in size 20x20x80 mm, thus a volume of 32 cm<sup>3</sup> and so a total

of 128 cm<sup>3</sup> is obtained. Once the slurry is poured, the mold is put in a furnace at 85°C and 100% relative humidity for 24 h, in order to complete the hydration process. The process allows to reach the complete hydration of Portland cement which would occur if it were left for 28 days at environment condition, as it is established by the standard criterion for cement resistance evaluation.

In order to estimate the precise quantity of cement to mix with water it is assumed that the total volume of the specimen ( $V = 128 \text{ cm}^3$ ) is equal to the sum of the volume of powder cement ( $V_c$ ) and the volume of water ( $V_w$ ):

$$V = V_c + V_w = \frac{M_c}{\rho_c} + \frac{M_w}{\rho_w} = M_c \cdot \left( \frac{1}{\rho_c} + \frac{w}{c} \right)$$

As a rule the quantity of cement is considered increased by a 10% since some material typically remains on the surface of the beaker during mixing. So considering the density of the cement and of the water respectively  $\rho_c = 3.15 \text{ g/cm}^3$  and  $\rho_w = 1 \text{ g/cm}^3$  and the total volume  $V = 128 \text{ cm}^3$ :

$$M_c = \frac{128}{\left( \frac{1}{3.15} + \frac{w}{c} \right)} \cdot 1.1$$

After curing in the furnace, the four specimen are unmolded and eventually cooled down. Since the w/c ratio is very elevated, the phenomenon of bleeding takes place and a thin layer of liquid water remains on the samples. This implies that not all the water theoretically considered in the hydration process has mixed with cement, so the theoretical w/c ratio is actually slightly lower than the actual w/c. From the past researches is pointed out the benefit in the addition of anti-setting agent: when it is not present, the density of the specimen reaches a plateau when w/c ratio is about 1 and do not decrease anymore even if the w/c ratio is increased, while when the anti-settling is present the decrease of the density is proportional to the increase of the w/c ratio.

Eventually after the unmolding the specimen are treated with a piece of sandpaper if there is the necessity to smooth them and eliminate some protrusions that could arise during the hydration in the furnace. Then they are measured by means of a mechanical caliper along the three dimensions and in order to have an accurate measurement three values are measured along each dimension at the two ends and in the centre, then the average is taken. The volume is thus obtained by the multiplication of the three dimensions measured. The other parameter needed to have the density is the mass, so the samples are weighed on a Radwag laboratory scale PS 510/C/1 (resolution of 1 mg). Two weights have been measured: one after the unmolding, this means cement hydrated at 85°C (temperature considered representative of a cycle charged by standard fat-plate solar collector), the second after a second curing cycle in the furnace kept at 140° C for an hour (representative of concentrated solar collector). Moreover keeping the samples in the furnace at 140°C allows a complete hydration of the paste. The density is obtained by the ratio of the mass of the hydrated cement (140°C) over the volume. The computation of the density is the key to evaluate the porosity of the samples. A simple analysis on the sample is about that the

lower is the density the higher the porosity, because it means that a lower weight is a symptom of a greater presence of voids inside the material.

The porosity is the main parameter to be considered in the choice of a material for a STES application, so it is the reason why the cement was preferred. To evaluate this parameter some considerations have to be underlined. From the past researches (18) has emerged that the bleeding phenomenon when dealing with high w/c ratio and the resulting actual w/c ratio, lower than the theoretical one, influences the porosity of the sample. Taking in account that the stoichiometric w/c ratio needed for the complete hydration of cement is 0.23, a mathematical formula to evaluate the porosity that theoretically is present in a hydrated cement can be recalled from (18):

$$p_{th} = \frac{\frac{w}{c} - \frac{1.14}{\rho_c} + 0.19}{\frac{1}{\rho_c} + \frac{w}{c}}$$

where  $p_{th}$  stands for theoretical porosity.

The procedure employed in this work to have an estimate of the porosity from an experimental point of view is the following: after weighing the completely hydrated cement at 140°C, thus having evaporated completely the residues of water still present, the samples are dipped in a bowl full of water until they are completely immersed. This causes the water to fill inside the pores of the cement and to replace the voids. The specimen are kept for some hours inside the bowl until no more bubble come out from them, leaving the time to the water to enter in the paste. Then they are taken out, dried with a damp cloth and then weighed. This corresponds to the third weighing at which our samples are subjected: it is clearly shown as the third value related to the wet weight is the higher because it represent the cement filled with water, while the one related to the complete hydrated cement at 140°C is the slighter. It is important to underline that this method is not completely accurate due to the presence of the “close porosity”, that indicates the presence of void inside the cement not connected to the surface of it, thus not reachable for the water or for the impregnation with hygroscopic salts, but well accounted in the calculation of the theoretical porosity. This implies that the experimental porosity is underestimated with respect to the theoretical one, even if for the didactic purpose of this work the “open porosity” is the one to take in account, because close porosity cannot be reached neither by the water neither by the salt or the vapor during the application, thus the one obtained with this method is considered a satisfactory estimation.

Naming  $M_{wet}$  the weight of the cement filled with water,  $M_{dry}$  the complete hydrated one, V the volume of the single sample, the porosity p (%) is estimated as:

$$p = \frac{(M_{wet} - M_{dry})}{\frac{\rho_w}{V}}$$

having considered  $\rho_w = 1 \text{ g/cm}^3$ .

## 4.2 impregnation

Once the percentage of porosity inside the samples is estimated, this is associated to the quantity of hygroscopic salts that can be inserted in the matrix to create the composite material for the STES applications. The purpose is to fill the cavities with a saturated solution of water and salt, then a further dehydration in the furnace is needed to make the water evaporated and thus to charge the composite material composed by cement and anhydrous salt.

The cement samples were divided in smaller pieces, typically 4 or 5 slides are made of the initial specimen, in order to facilitate the saturated solution to fill in the pores and so the salt to enter the cavities of the matrix. Then they undergo a full dehydration process in the furnace at 140°C for 1 hour with the aim of eliminate any trace of water, since cement is a porous material and some humidity from the environment can penetrate inside.

An amount of saturated solution is prepared taking into account that the quantity ( $V_{sol}$ ) to enter in the piece of the cement is equal to the percentage of pores ( $p$ ) multiplied by the volume of the slice ( $V_{slice}$ ), found by means of the ratio between the mass of the slice and the density of the sample formerly calculated, with the assumption that the entire sample and the little portion of it share the same density:

$$V_{pores} = V_{sol,1} = p \cdot V_{slice} = p \cdot \frac{M_0}{d_{sample}}$$

The solution is drawn in a pipette and slowly dropped in the slices . In this phase some difficulty came to light: the cement is not able to absorb all the estimated quantity of solution and some liquid in excess do not enter the pores but remains out of the sample. One reason could be that in the solution a poor part of the salt precipitates in crystal, thus do not reach the cavity of the cement that is reached by water. Another motivation is that the dimensions of pores could be modified over the time because of the environmental conditions, so despite the dehydration phase in the furnace, the actual volume of pores could be inferior with respect the one estimated through calculations.

Following the impregnation, the samples are dried in the furnace at 85°C for 1 hour, the water evaporates and the anhydrous salt remains in the matrix. A thin layer of salt is visible on the samples and nearby them, this represents the portion of solution that do not reach the cavity of the pores. With the aim of evaluate the quantity of salt inside the sample, this method, based on the weight uplift due to the solution that filled in the cement, is applied: the sample, after the drying in the furnace subsequent the impregnation, is weighted and the value called  $M_1$ . This value is compared with the weight in the dehydrated pure cement condition  $M_0$ . The quantity resulted can be estimated with the weight of the salt ( $M_{salt,1}$ ) spread in the sample:

$$M_{salt,1} = M_1 - M_0$$

Consequently its volume, with the assumption that the salt in the matrix is in the anhydrous condition, is:

$$V_{salt,1} = \frac{M_{salt,1}}{\rho_{salt}}$$

Taking as  $\rho_{salt}$  the density of  $MgSO_4 = 2.66 \text{ g/cm}^3$ .

In that way it is clear that the volume of pores initially estimated is not fully exploited, thus it is possible to repeat the procedure more times with the objective to increase the quantity of anhydrous salt in the sample. In this work some samples are impregnated a second time considering the volume of solution to introduce equal to the volume of pores that remains void:

$$V_{sol,2} = V_{pores} - V_{salt,1}$$

As it happened in the first impregnation, also in the second not all the theoretical  $V_{sol,2}$  is introduced in the sample producing a situation in which a thin layer of salt remains on the surface of the sample, meaning that is not penetrated inside the matrix and therefore easily dissoluble at the first application.

Although this inconvenience, a further amount of salt is inserted in the matrix and thus it could be estimated. Then the calculation for the estimation of salt inside the matrix is repeated as the previous one of the first impregnation. Calling  $M_{salt,2}$  the mass of salt introduced with the second impregnation,  $m_2$  the weight of the sample after the second curing process in the furnace for 1 hour at  $85^\circ\text{C}$  subsequent the second impregnation:

$$M_{salt,2} = M_2 - M_1$$

Finally a rough estimation of the density of the composite material after the impregnation can be computed, taking the ratio of the weight of the sample after the second impregnation  $m_2$  divided by the volume of the sample. Moreover a theoretical concentration of anhydrous salt inside the matrix is estimated as:

$$sf = \frac{M_{salt,2} + M_{salt,1}}{M_{salt,2} + M_{salt,1} + M_0}$$

where  $sf$  stands by salt fraction.

### 4.3 in situ

The in situ synthesis in an innovative procedure that has the aim of spreading hygroscopic salts directly in the cement matrix during the mixing with the powder. It consists in preparing the cement paste employing directly the solution of water and salt instead of pure de-ionized water. The advantage is to embed and distribute uniformly the salt inside the hosting matrix, eliminating the risk of loss or leakage that could occur during the utilization when the composite material is produced inserting the salt inside the matrix with the impregnation (18).

The production start with the mixing of the solution composed by salt and water, taking in account the solubility in the water of the two salts chose for this work. Then the blending of the solution and the cement powder takes place with the mechanical stirrer.

It is important to note that in the in situ synthesis the quantity requested to mix the solution and the cement cannot follow the stoichiometric rule of w/c ratio because when salt reacts with water some hydrates are produced. Thus a portion of the whole quantity of water involved in the solution chemically bonds with the salt, while only the remaining portion is free to react with the cement. Some assumptions are now formulated differently for the two employed salts in order to estimate the quantity of water in the solution free to bond with the cement and so to give a valuation of the w/c ratio to employ in an in situ synthesis. This is due to the difficulty of establishing precisely the hydration degree of the compound in the saturated solution and successively its evolution during the mixing with the cement and also the modification that undergoes in the curing process. The result is an estimation of the density and of the concentration of salts inside the matrix that can be considered truthful for a comparison between the different products of the in situ synthesis.

When a saturated solution is produced with  $MgSO_4$  and  $CaCl_2$ , it must be considered which hydrate is generated, since both the salts present several types of hydration precipitations. Working with the magnesium sulfate, it is to precise that in this research it is employed directly the epta-hydrate  $MgSO_4 \cdot 7H_2O$  that is stable at room temperature, thus being the salt already hydrated and having a solubility in water of 113g/100mL, it is assumed that all the quantity of water that participate at the saturated solution reacts with the cement. Naming as  $M_c$  the mass of cement,  $M_w$  the weight of water and  $M_{MgSO_4}$  the quantity of  $MgSO_4 \cdot 7H_2O$ , both mixed in the saturated solution, the samples are produced considering:

$$\frac{w}{c} = \frac{M_w}{M_c}$$

$$\frac{s}{c} = \frac{M_{MgSO_4}}{M_c}$$

where s/c is the weight ratio between salt and cement.

The other parameters needed to characterize this sample are the one taken by (18): theoretical density  $d_{th-salt}$ , theoretical porosity  $p_{th-salt}$  and salt fraction  $sf_{th-salt}$ :

$$d_{th-salt} = \frac{1 + \frac{w^*}{c} + \frac{s}{c}}{\frac{1}{\rho_c} + \frac{\frac{w}{c} + \frac{s}{c}}{d_{sol}^*}}$$

$$p_{th-salt} = \frac{\frac{\frac{w}{c} + \frac{s}{c}}{d_{sol}^*} - \frac{1.14}{\rho_c} + 0.19}{\frac{1}{\rho_c} + \frac{\frac{w}{c} + \frac{s}{c}}{d_{sol}^*}}$$

$$sf_{th-salt} = \frac{\frac{s}{c}}{1.23 + \frac{s}{c}}$$

where  $w^*/c$  is the stoichiometric ratio needed for the complete hydration of cement and is equal to 0.23, while  $d_{sol}^*$  is the density of the solution of salt into water.

The difficulties encountered dealing with magnesium sulfate is its very fast settling time when mixing the saturated solution with cement powder. This requires  $w/c$  ratio extremely high (minimum 1.7 as experimented) and the cement powder has to be poured slowly, as well as the rotational movement of the stirrer has to be mild.

Different is the assumption dealing with calcium chloride. In the laboratory was employed  $CaCl_2$  not hydrated, so in order to apply the ratios  $w/c$  and  $s/c$  it has to be considered the hydration that takes place in the saturated solution. It is assumed that calcium chloride precipitates in its hexahydrated form  $CaCl_2 \cdot 6H_2O$ , producing thus six hydrates incorporated in the crystal lattice. Thus starting from the solubility of  $CaCl_2$  in the water that corresponds to 74.5g/100mL, considering the moles that operates in this solubility ratios and separating the moles of water needed to form hexahydrate crystals from the ones free to mix with cement, it can be roughly stated the quantity of water that can be exploited in the  $w/c$  ratio. Once  $w/c$  is computed, from the total quantity of solution it can be stated also  $s/c$  and  $d_{sol}^*$ , and with the same formulas already seen for the magnesium sulfate, the parameters of theoretical density, porosity and salt fraction are calculated.

## 4.4 in situ impregnated

The in situ synthesis samples after being dehydrated in the furnaces present a discrete amount of porosity so they can be impregnated with the same procedure applied for the cement samples. The obstacle in this procedure is that it is impossible to perform the calculation of the experimental porosity with the same method adopted for the cement samples, that is to dip the specimen in the water in order to fill the pores, for the risk of disintegrating the products.

Thus instead of estimate the quantity of solution to infiltrate in the sample starting from the porosity of the sample before the loading process, here a standard amount of solution is dropped on the material, generally around 2 ml of saturated solution. Then, having weighed the standard amount of solution infiltrated, the quantity of salt entered in the sample is calculated as showed in the paragraph 4.3.

As explained before, after the first loading the sample is dried in the oven for 1 hour at 85°C and then it can be impregnated a second time. After that, knowing the quantity of saturated solution employed in both the loading process, the properties like density and salt fraction can be calculated.

## 4.5 preliminary thermal test

The composite materials produced, both with impregnation and in situ synthesis, undergo a “preliminary thermal analysis” in the DISAT laboratory to prove the effectiveness of the production methods and to highlight the most promising specimen.

The experimental setup consists in small cylindrical chamber insulated by a layer of polystyrene in which the sample (with the role of the sorbent) and liquid water (sorbate) enter in contact and the sorption reaction can occur. The chamber is filled with water in a quantity of about 10mL, then the sample in the form of small pellet of about 3-4g is inserted trying to keep it completely under the water level. The sample are formerly dehydrated in the furnace for 1 hour at 140°C, simulating the working temperature of the modern solar panels and completing the dehydration process that make the water evaporate and the salt to be present in the anhydrous form. Then the chamber is closed by a little plastic lid in order to insulate the sorption mechanism.

The temperature variation is detected by a K-type thermocouple (Chromel (Ni-Cr) (+) / Alumel (Ni-Al) (-)) that send the information to a data logger connected to a pc that via software continuously plot and collect the temperature. A weighed amount of water is poured in the hole, the temperature is measured, named initial temperature  $T_i$ , with the thermocouple until it stabilize around the value of the environmental temperature. Then the dehydrated small pellets of material is weighed and dipped in the water, the chamber is closed, and the sorption process starts. Generally the sorption systems employ water in the vapor state, but for the aim of this test, which is only to skimming the best materials from the worst ones, it is a good compromise to facilitate it exploiting liquid water. The rise of the temperature due to the released heat of the sorption mechanism is detected by the thermocouple and the experiment goes on until it reach to decrease or remains stable, collected as final temperature  $T_f$ .

Identifying the rise of temperature inside the chamber it is possible to estimate the energy content stored in the samples with the formula:

$$E = \Delta T \cdot \sum m_i \cdot cp_i$$

Where are considered the mass of the samples tested  $m_i$  and the specific heat taken as a summation of the heat capacity of the single values of the components multiplied by the respective amount of mass in the sample.

As far as this calculation may seem profitable in defining the composite material produced, actually this experiment presents some limitations. The chamber in which the reaction takes place allows to insert only a small amount of water and material, so the rise of temperature experienced is limited by this small contribution of masses. Moreover it should be pointed that for the success of the experiment it should starts with the sorbate and sorbent at thermal equilibrium, but the thermocouple allows only to measure the initial temperature inside the chamber, precisely the water (the sorbate) at environmental temperature, while the one of the sorbent is only assumed to be the same.

It is fundamental to underline that the energy measured with this experiment set up is not sufficient to estimate the real energy released by the sample. This is because the released heat in the thermal reaction in the chamber warms the water and a small amount of it evaporates. It corresponds to the enthalpy of vaporization, the amount of energy that must be added to a liquid substance to transform a quantity of that substance into a gas, phenomenon that happen at constant temperature. So in this situation a rise of temperature is not experienced and it

generates a slightly underestimation of the final temperature. To have a complete measurement of the total energy released in the reaction is needed to detect the water uptake of the sample, that will be performed in the INRIM laboratory.

The only aim of this experience is to have an idea of the effectiveness of the production method and to have a partial skim of the best material under the thermal point of view. It turns out that the in situ samples produced with the sulfate magnesium are the most promising one because provides the widest rise of temperature.

## 4.6 sorption analysis

in this chapter is described the methodology adopted to analyze the thermal properties of the composite material produced in terms of stored energy. To achieve this objective it is needed to plot the adsorption isotherms from which the main properties of the material can be extracted. The test is performed at INRIM, in a climatic chamber named 'Model 2500 Benchtop Humidity Generator', from Thunder Scientific Corporation, with chamber humidity and temperature uncertainties at setpoint of 0.5%RH and 0.06°C (and temperature uniformity of 0.1°C).

The aim of this test is to plot the adsorption isotherms obtained by charging the sample in the climatic chamber at a constant temperature under the effect of a variable partial pressure, procured with a flow of air mixed with vapor that corresponds to the relative humidity set in the chamber. The partial pressure can be calculated as follows:

$$p = RH \cdot p_s$$

Being  $p$  partial pressure,  $p_s$  the saturation pressure and  $RH$  the relative humidity set on the machine.

The parameters needed to plot the isotherms are the relative humidity and the weighed water uptake of the samples. The constant temperature at which the experiment is set up are 30°C and 50°C, and the relative humidity is set up to 5 levels, specifically 10-30-50-70-90%.

At the beginning the samples have to be pelletized and dried at 140°C for several hours. They are weighed until the drop of mass reach a stability level, named  $M_0$ , that means that the pellets are constituted by a matrix of cement with anhydrous salt dispersed inside. Then they are situated in small circular aluminum pans which are arranged inside the climatic chamber at 50°C and 10% RH, that corresponds to the first level of the measurement. At this point the vapor flows inside the chamber and the samples adsorb it, increasing the mass. It is important to let the cement to reach the saturation point, i.e. the weight at which the vapor can no more flows inside the pores because the sample is completely hydrated. This is a slow process, so in order to allow it to be completed, the specimens are left inside the chamber for 24 hours for each of the relative humidity at which they are tested, time considered reasonable to let the process finish.

After that amount of time, the pan of each sample is taken out from the chamber and weighed, named  $M_{RH}$ . Since environment and chamber are at different conditions of temperature and

humidity, the passage of opening the chamber and weighing the samples has to proceed as fast as possible, in order to not alter the condition inside the machine. Fortunately only two specimens are tested, this facilitate the speed at which the weighing proceeds. After having weighed the samples at 50°C and 10%RH, the chamber is set at the next level of relative humidity, the pans with the cement above are laid inside and left for another 24 hours.

After this process the water uptake, named the load  $x$ , is calculated as follows:

$$X = \frac{m_{water}}{m_{sorbent}} \Big|_T$$

where with  $m_{sorbent}$  is intended the dry mass of the sample,  $M_0$ , while for  $M_{water}$  is intended the vapor mass adsorbed by the sample for each level of RH at the constant temperature, i.e.:

$$M_{water}(RH, T) = M_{RH, \%} - M_0$$

Once the mass of the samples kept at 50°C and 90%RH are taken, the chamber is set at 30°C in order to plot the second isotherm and 10%RH to restart the measurement. Prior to this, the samples are dried again at 140°C, and the process is concluded after keeping them at 30°C and 90%RH, the last level of the experiment.

## 4.7 the Brunauer–Emmett–Teller (BET) modeling

The data collected in the Table 4.1 are plotted in a pression [mbar]/ load [g/g] graph and they resembles the shape of the type II isotherms according to the IUPAC classification. These isotherms are generally described by the theory developed by S. Brunauer, P. H. Emmett and E. Teller called BET theory (28), that describes the mechanism of adsorption of gases in multimolecular layers.

They identified three zones in the S-shape isotherm: a short concave zone with respect pressure axis at the lower zone, a semi-linear portion starting at the “knee” and a larger high pressure convex zone. The BET theory identifies the “knee” of the isotherm with the completion of the monolayer coverage, i.e. the moment in which the gaseous particles are considered adsorbed on the unique layer of the adsorbent. The semi-linear zone is associated to the beginning of the multilayer covering process, while the convex area with respect to the pressure axis is lead by the capillary condensation occurring at the core’s pores.

The BET model it is chosen to fit with the experimental data and to show if the theory of multimolecular layers could be applied to this case. In the work a formula is presented:

$$v = \frac{v_m * c * p}{(p_0 - p) * (1 + (c - 1) * \left(\frac{p}{p_0}\right))}$$

This formula represent the total volume  $v$  adsorbed. The meaning of the other terms are:

- $v_m$  is the volume of gas adsorbed when the entire adsorbent surface is covered with a complete unimolecular layer.
- $c$  is an adimensional quantity that suggests the strength of the interaction between water and sorbent and the value is generally larger than unity when the curve corresponds to an S-shape isotherm, while it could be absent in the case of isotherm III.
- $p_0$  is the saturation pression

If  $\frac{p}{p_0} = x = RH$ , the formula becomes :

$$v = \frac{v_m * c * p}{(1-x) * (1-x+cx)}$$

The volume  $v$  and  $v_m$  can be preferably expressed as  $n$  and  $n_m$  moles per gram. Hence  $n_m$  represent the point at which the curve becomes semi-linear and  $c$  characterizes the shape of the “knee”.

This formula resulted to not be suited to describe the steepest zone of the S-shape isotherms, i.e. when  $RH > 50\%$  and the curves tend to become convex with respect the pressure axis. Thus a more general definition of the formula is developed, considered a finite number  $N$  of layers and no more an infinite number of them:

$$v = \frac{v_m * c * p}{(1-x)} * \frac{1 - (N+1)x^N + Nx^{N+1}}{1 + (C-1)x - Cx^{N+1}}$$

A traditional fitting through minimization of the root mean square error (RMSE) was followed to fit the experimental data with the formula of the BET theory, while varying the parameters in the proper range ( $c > 2$ ,  $N \in \mathbb{N}^+$ ,  $v_m$ ).

	Sample	m0 [g]	m10 [g]	m30 [g]	m50 [g]	m70 [g]	m90 [g]
T = 50C°	Mg18	16,209	17,123	17,446	17,746	18,038	18,472
	Mg08 2 impr	22,638	23,785	24,155	25,613	25,95	31,227
T = 30C°	Mg18	16,493	17,394	17,716	17,959	18,164	18,546
	Mg08 2 impr	22,814	23,861	24,893	26,16	26,934	29,227

Table 4.1– Experimental water uptake of the samples in the climatic chamber

## 4.8 sorption properties evaluation

The main heat storage properties needed to evaluate the composite material produced are the cycled heat  $Q_u$  [MJ/kg] and the energy density  $E_d$  [GJ/m<sup>3</sup>], which represent the energy per unit of volume that the material can store. It is important to note that these properties are strictly related to the environmental and working conditions. Thus, in order to perform the calculation, it is simulated that the material operates in a closed loop system with well defined boundary conditions, i.e. the working temperature of the solar collector that is considered in the range 140-150°C with the aim to heat a domestic space at an appropriate temperature. In this paragraph it is resumed the methodology followed to estimate the properties, the results and the values in which the operating cycle are reported in the paragraph 5.3.2.

Considering the Clapeyron chart ( $-1/T$ ,  $\ln(p)$ ) several isosteres are necessary to evaluate the thermodynamic cycle and the methodology to obtain them is to starting from the adsorption isotherms of all the temperatures between the boundary conditions of the system, i.e. that one of the heating appliance used, typically about 40°C for a domestic or working room, and that of the operating solar panel 150°C.

Since the data collected in the climatic chamber are obtained for only two isotherms (30°C and 50°C), the Polanyi potential theory is applied to obtain the needed isotherms from the available data. This theory, that lies on the base of very popular empirical equations proposed by Dubinin and co-workers, considers the absorption process to be similar to the condensation and that the absorbed state behaves similar to a liquid. In this scenario, the principle of temperature invariance declares that, at different temperatures  $T_1$  and  $T_2$ , equal uptake can be achieved at the gas pressures  $p_1$  and  $p_2$  which are linked as:

$$T_1 \ln\left(\frac{p_0}{p_1}\right) = T_2 \ln\left(\frac{p_0}{p_2}\right)$$

It is thus assumed a direct correspondence between the adsorption uptake and the product  $T \ln\left(\frac{p_0}{p}\right)$ .

Dubinin introduced a similar value  $A_{dub} = \Delta F = -RT \ln(p_0/p)$  [J/mol] called “adsorption potential”, expressed as the negative of the free energy of adsorption variation. The main advantage of this term is that the equilibrium uptake, considered as the adsorbed load  $\Delta x$  [g/g], can be expressed as a unique function of the single variable  $A_{dub}$ , instead of usually employs both parameter  $p$  and  $T$ :

$$\Delta x \propto f(A_{dub})$$

Thus on a  $A_{dub} - \Delta x$  graph it can be plotted the experimental load and obtain a “characteristic sorption curve” presented as function of  $A_{dub}$  and independent by the temperature or pressure used. Having the characteristic sorption curve as starting point, any isotherm or isobar can be derived by sampling the curve at the desired potential linked to the values of  $p$  and  $T$ .

To fit the experimental data in a characteristic curve the 'Curve Fitter' application of matlab is employed. This is a toolbox that provides an interface where it is possible to fit curves and surfaces to data, to plot and to compare multiple fits, to choose between different interpolation and smoothing methods. Among the several interpolation method, the one that provides the smoother and the most accurate fitting is selected.

As explained, by sampling the characteristic curve at a given potential linked to the desired temperature, every isotherm could be plotted on the (P [mbar], x [g/g]) graph.

The different obtained isotherms are necessary to derive the isosteric curve on the clapeyron chart from which the cycled heat ( $Q_u$ ) and the energy density ( $E_d$ ) can be extracted.

The relationship between temperature and adsorption pressure is related to the definition of the isosteric heat,  $q_{is}$ , as:

$$q_{is} = R \left( \frac{\partial \ln p}{\partial (-\frac{1}{T})} \right) \text{ at } x = \text{const}$$

It can be approximated to the slope of the driest isostere in the cycle multiplied by R:

$$q_{is} = R \left| \frac{\Delta P}{\Delta T} \right|$$

To calculate the cycled heat  $Q_u$  [MJ/kg], which corresponds to the heat that the system can deliver per unit of mass of the dry sorbent, the isosteric heat has to be multiplied by  $\Delta x$ , i.e. the water uptake achievable by the given cycle, typically lower than the maximum water uptake of the material, and divided by the water molecular mass  $MM_{H_2O}$ , namely 18.0153 g/mol:

$$Q_u = \frac{q_{is} \Delta x}{MM_{H_2O}}$$

It is important to underline the thermal boundary conditions of the closed loop system considered to evaluate the properties:

- $T_w$ , the average winter temperature taken as 10°C
- $T_s$ , the average summer temperature taken as 30°C
- $T_A$ , the heat sink temperature, chosen as 40°C in order to maintain a warm climate inside the domestic room
- $T_C$ , the heat source temperature, considering the one of the concentrated solar panel to be around 150°C

Once the saturation line is plotted in the clapeyron chart considering the two points of winter ( $-1/T_w; \ln(p_{0w})$ ) and summer ( $-1/T_s; \ln(p_{0s})$ ), the point A and C of the cycle are fixed, given the boundary conditions and that their ordinates correspond to the saturation vapor pressure of water at respectively  $T_w$  and  $T_s$ . Having point A ( $T_A, p_A$ ) and C ( $T_C, p_C$ ), the adsorption potential  $A_{dub}$  can be obtained, then following the characteristic curve a value of  $\Delta x$  is determined and this

allows to have the isosteric in the clapeyron chart. The difference between the bigger and the smaller isostere of these two operating points provides the water uptake achievable by the thermodynamic cycle.

Lastly the energy density ( $E_d$ ) can be obtained multiplying the cycled heat ( $Q_u$ ) by the density of the dried composite (dried at 140°C):

$$E_d = Q_u \cdot d_{140^\circ C}$$

## 5. Results and discussions

The results of the tests are shown in this section, focusing on the thermal properties that have been successfully achieved in relation with the percentage of salt content included in the sample. A brief recap on the density and porosity of the pure cement based samples is only to highlight what is the well-known trend that porosity increases when the density decreases and this is achieved acting on the w/c ratio. The larger is the ratio, the more porous is the sample, the more salt can be included inside and the more effective the sorption phenomenon is. For this reason all the pure cement samples has been produced with w/c ratio of 1, 1.5 and 2 in order to maximize the porosity.

### 5.1 salt content

The composite materials are produced with both salt loading technique and in situ synthesis. Also a combination of in situ samples that undergoes impregnation has been produced. The salts employed are  $\text{CaCl}_2$  and  $\text{MgSO}_4$ . It must be pointed out that some difficulties arised in the mixing of cement powder and saturated solution of  $\text{MgSO}_4$  during the in situ synthesis due to the elevate and rapid settling of the slurry phase. This leads to the utilization of a small quantity of cement and a very high quantity of solution, thus obtaining very high values of w/c and s/c, as shown in the last part of Table 5.1. However the samples show a proper hardening after the curing in the furnace and remains compact and robust although the high level of liquid solution employed. The same problem does not occur in the  $\text{CaCl}_2$  products, even if this kind of samples experience the issue of the deliquescence typical of this salt as it is explained in the paragraph 5.3.

The Table 5.1 resume the density and salt percentage fraction reached by the samples, by specifying whether it is an in situ synthesized or an impregnated one and the eventual cycles of impregnation it has undergone.

Impregnation with MgSO <sub>4</sub>	w/c	N° impr	density	Salt fraction
			[g/cm <sup>3</sup> ]	[%]
310_1B	1	1	1,065	26,2
310_15B	1,5	1	1,076	35,5
422_15C	1,5	1	1,023	32,4
525_2C	2	1	1,24	35,5
608_15A	1,5	1	1,17	19
310_1D	1	2	1,23	30
310_15D	1,5	2	1,092	45
422_15D	1,5	2	1,35	40
525_2B	2	2	1,36	42
608_15B	1,5	2	1,28	24,5

Impregnation with CaCl <sub>2</sub>	w/c	N°impr	density	Salt fraction
			[g/cm <sup>3</sup> ]	[%]
310_1C	1	1	1,29	30
310_15C	1,5	1	1,08	42
310_1A	1	2	1,54	38,5
310_15A	1,5	2	1,25	51,5
422_15B	1,5	2	1,58	47
525_2A	2	2	1,06	51

In situ	w/c	s/c	density	Salt fraction
			[g/cm <sup>3</sup> ]	[%]
Mg08	1,71	1,94	1	61
Mg18	2	2,26	0,95	65
Ca13	0,65	0,826	1,4	40
Ca20	1	1,29	1,2	51

In situ impregnated	w/c	s/c	N°impr	density	Salt fraction
				[g/cm <sup>3</sup> ]	[%]
Mg08_A	1,71	1,94	2	1,49	67
Mg08_B	1,71	1,94	2	1,45	66,6
Mg08_C	1,71	1,94	1	1,39	66,7
Ca13_C	0,65	0,826	1	1,6	50
Ca13_B	0,65	0,826	2	1,635	58
Ca20_A	1	1,29	1	1,378	61
Ca20_B	1	1,29	2	1,4	58
Ca20_D	1	1,29	2	1,41	56

Table 5.1 – Levels of salt fraction and density obtained in the production of the different samples.

On one hand, regarding the pure cement samples impregnated with salt, it could be assumed a theoretical trend for which at higher w/c ratio corresponds higher porosity and thus higher percentage of salt fraction that can be included inside, but the experimental results do not show this predictable trend. The causes that may be at the base of this different behavior of each single sample could be various: for example the dissimilar viscosity of the pure water used as means to evaluate porosity and the saline solution, or the potential precipitation of salt crystal that may block the access to the pores. Dissimilar and without following a clear path will be also the energy released by each impregnated sample, as it will be presented in the next paragraph.

On the other hand, it is clear that the greater salt fraction is obtained by the in situ process and it is risen by the impregnation, reaching a peak of about 67% of  $MgSO_4$ . The samples produced with magnesium sulphate present the higher amount of salt content due to the great porosity, even though this is a property that cannot be estimated with the technique of dipping them inside a batch of water due to the high risk of deliquescence of the salt inside the matrix. An index of the porosity of the in situ synthesized is the density, recalling the well-known inverse proportionality of these two parameters. Comparing the in situ samples it is shown that the density of the  $CaCl_2$  compound is higher than the  $MgSO_4$  one and accordingly to that their porosity is slightly lower. For this reason the salt fraction inside the  $MgSO_4$  samples resulted to be higher compared with the others.

## 5.2 Preliminary thermal analysis

The table 5.2 shows the estimated values of energy density of the samples and the rise of temperature recorded. Every sample has been pelletized in order to match the dimension of the cylinder where they are tested and to do at least 2 or 3 trials for the same specimen.

samples	in situ	N°impr	salt	$\Delta T$ [K]	E [GJ/m <sup>3</sup> ]
310_1B	no	1	$MgSO_4$	1,9	0,042334
310_15B	no	1	$MgSO_4$	2,5	0,1076
310_15D	no	2	$MgSO_4$	2	0,090188
310_1D	no	2	$MgSO_4$	1,5	0,04396
422_15D	no	2	$MgSO_4$	2	0,04611
422_15C	no	1	$MgSO_4$	2,5	0,047496
525_2B	no	2	$MgSO_4$	2	0,046076
608_15B	no	2	$MgSO_4$	1,9	0,047835
608_15A	no	1	$MgSO_4$	1,2	0,026655
525_2C	no	1	$MgSO_4$	1,5	0,036756
310_1A	no	2	$CaCl_2$	1,1	0,02936
310_15C	no	1	$CaCl_2$	2,8	0,128555
310_1C	no	1	$CaCl_2$	0,7	0,037023
310_15A	no	2	$CaCl_2$	1,4	0,039463
422_15A	no	1	$CaCl_2$	2	0,049484

<b>422_15B</b>	no	2	<i>CaCl<sub>2</sub></i>	3	0,069258
<b>525_2A</b>	no	2	<i>CaCl<sub>2</sub></i>	2,7	0,066059

Table 5.2 – Energy density obtained for the impregnated samples in the preliminary thermal test

All the samples produced with the salt load technique exhibits a rise of temperature in the range of 1÷3 K and a energy density below the 0.05 GJ/m<sup>3</sup>, regardless if they are loaded with CaCl<sub>2</sub> or MgSO<sub>4</sub>. The high variations experienced by the samples 310\_15B, 310\_15D and 310\_15C when the energy released reaches the peak of 0.1 GJ/m<sup>3</sup> can be explained because a little amount of material underwent the treatment with respect to the usual quantity exploited, respectively were exercised 0.7, 0.75 and 0.43g of material, while the average weight of sample tested is about 2 grams.

<b>samples</b>	<b>in situ</b>	<b>N°impr</b>	<b>salt</b>	<b>ΔT</b>	<b>E</b>
				[K]	[GJ/m <sup>3</sup> ]
<b>Mg18</b>	si	0	<i>MgSO<sub>4</sub></i>	2	0,0372
<b>Mg08_A1</b>	si	2	<i>MgSO<sub>4</sub></i>	2,8	0,104217
<b>Mg08_A2</b>	si	2	<i>MgSO<sub>4</sub></i>	3,9	0,0949
<b>Mg08_A3</b>	si	2	<i>MgSO<sub>4</sub></i>	4	0,103988
<b>Mg08_B1</b>	si	2	<i>MgSO<sub>4</sub></i>	3,8	0,102336
<b>Mg08_B2</b>	si	2	<i>MgSO<sub>4</sub></i>	3,2	0,1024
<b>Mg08_B3</b>	si	2	<i>MgSO<sub>4</sub></i>	5	0,156401
<b>Mg08_C1</b>	si	1	<i>MgSO<sub>4</sub></i>	2,4	0,075337
<b>Mg08_C3</b>	si	1	<i>MgSO<sub>4</sub></i>	1,7	0,071444
<b>Ca20_2A</b>	si	2	<i>CaCl<sub>2</sub></i>	3,1	0,068185
<b>Ca20_2B</b>	si	2	<i>CaCl<sub>2</sub></i>	2,4	0,058416
<b>Ca20_2D</b>	si	2	<i>CaCl<sub>2</sub></i>	2,5	0,056259
<b>Ca13_15A</b>	si	2	<i>CaCl<sub>2</sub></i>	1,2	0,049455
<b>Ca13_15B</b>	si	2	<i>CaCl<sub>2</sub></i>	2,2	0,063929
<b>Ca13_15C</b>	si	1	<i>CaCl<sub>2</sub></i>	1,7	0,049437

Table 5.3 – Energy density obtained for the in-situ samples in the preliminary thermal test

For the in situ synthesized samples there are big differences, regarding the energy released, between the behavior of the magnesium sulphate and calcium chloride. The samples produced with saline solution of  $\text{CaCl}_2$  and impregnated with the same solution experienced an energy density of about  $0.05\div 0.06 \text{ GJ/m}^3$ , not so much higher than respect to the pure cement samples loaded with this salt. The low quantity of energy released combined with the problem of deliquescence of the calcium chloride in contact with water leads to discard them from the sorption test.

On the contrary, a double impregnation of the samples produced with a saline solution of  $\text{MgSO}_4$  produced very high values of rise of temperature ( $3\div 5 \text{ K}$ ) and energy density that reaches a peak of  $0.15 \text{ GJ/m}^3$  with the sample Mg08\_B3.

These preliminary thermal results suggest that the most worthy and promising materials to further test are the in-situ synthesized with  $\text{MgSO}_4$ , while the hygroscopic salt  $\text{CaCl}_2$  turns out not to improve effectively the thermal storage properties of the material.

In order to establish precisely the thermal properties of the in situ materials produced with  $\text{MgSO}_4$ , the sample Mg08, impregnated two times, and the pure in situ synthesized Mg18 without any salt loading are tested in a specific sorption analysis. For the completeness of the purpose of this work also the in situ sample Ca20 produced with  $\text{CaCl}_2$  is further tested in order to seek confirmation of the inefficiency of this salt under the thermal storage point of view.

## 5.3 sorption test

In this section the results of the sorption test carried out at the INRIM are presented.

During the test inside the climatic chamber the sample of in situ calcium chloride Ca20 resulted in a failure due to the high deliquescence of this salt, which spilled out from the pellets when the chamber was set at  $50^\circ\text{C}$  and the RH condition passed from 30 to 50. When the relative humidity of the environment exceeds the critical relative humidity, properties that depends on the material and the temperature, the salt absorbs water and dissolves. This results in an additional sorption of water and in an increase of the released heat, but with the risk of influencing the hosting material and, as in that case, spilling out from the matrix (29).  $\text{CaCl}_2$  presents a DRH very lower with respect to  $\text{MgSO}_4$ , it means that at equally temperature, it tends to be in a solution state at lower level of RH. With the increase of temperature, the DRH decreases, thus at  $50^\circ\text{C}$  and with a RH of 50%, the host matrix was not able to retain the salt solution that spilled out.

The results reported in this paragraph refer to the composed materials Mg18 and Mg08 both produced with  $\text{MgSO}_4$ .

### 5.3.1 BET fitting results

The experimental data of the vapor uptake in the samples at the different relative humidity conditions and temperatures are reported in the figure below, with the data fitting achieved by means of the BET theory. Each graph in the Figure 5.1 represent the load of the samples at each

temperature (30°C and 50°C), expressed as a function of the relative humidity. The parameter obtained through the root mean square error fitting procedure  $c$ ,  $N$  and  $nm$  are shown in the Table 5.4.

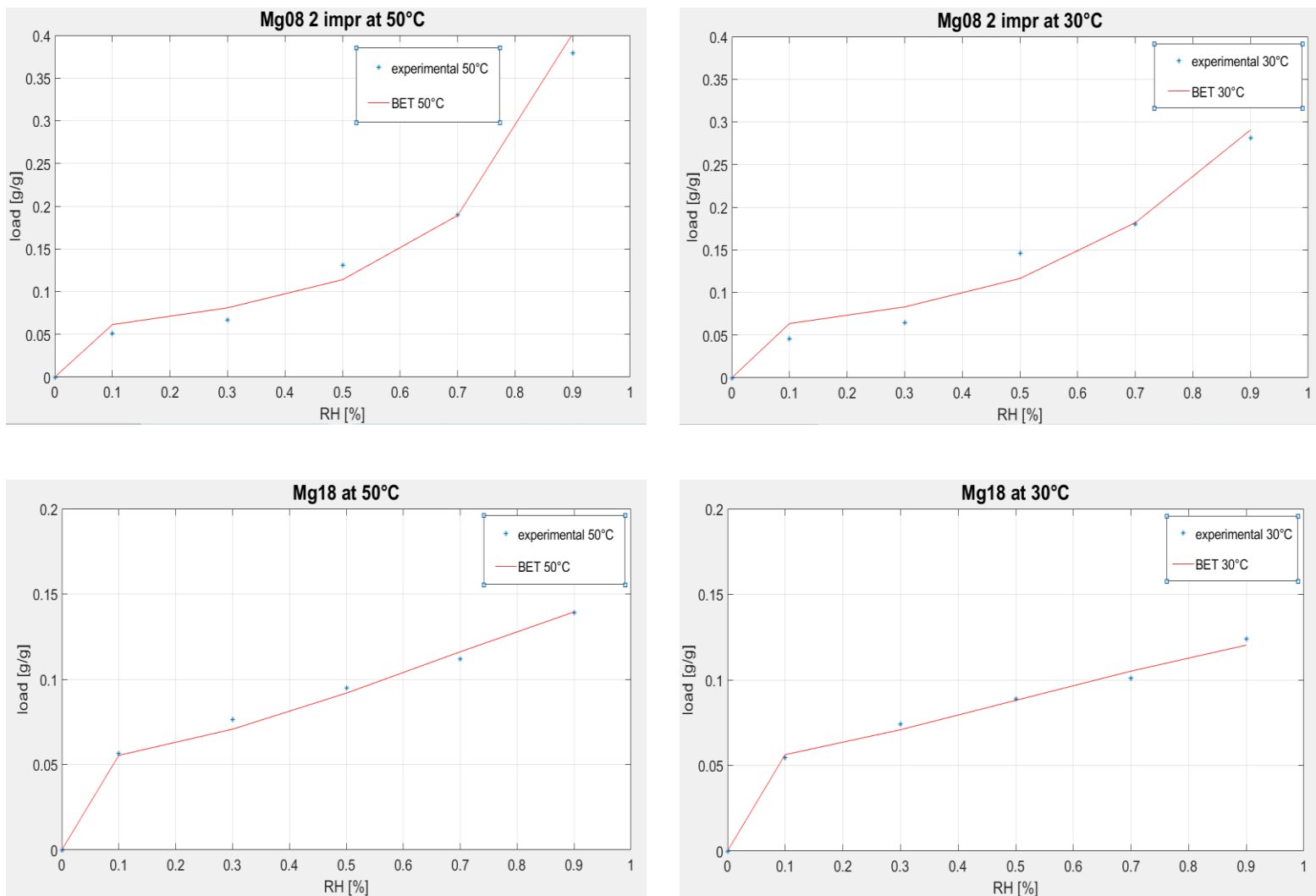


Figure 5.1 - BET model fitting of experimental data for the different samples at 50°C and 30°C

	30°C isotherm			50°C isotherm		
	C	N	nm	C	N	nm
Mg18	4060	4	0,0508	3074	5	0,0499
Mg08	394	11	0,0585	256	19	0,0572

Table 5.4 – Parameters for the BET fitting procedure

### 5.3.2 sorption properties evaluation

To plot the characteristic sorption curve two different interpolation methods are employed using the toolbox 'Curve Fitter' of matlab respectively for the two samples Mg18 and Mg08.

The most accurate interpolation results to be relying on the function load (Fig.5.2):

$$y = \frac{a}{(x + b)^c}$$

The 4 calculated parameter are reported in the table 5.5:

	a	b	c
Mg18	1500	4369	1.11
Mg08	280,8	612,2	0.9936

Table 5.5 – Parameters of the fitting function curve for the samples

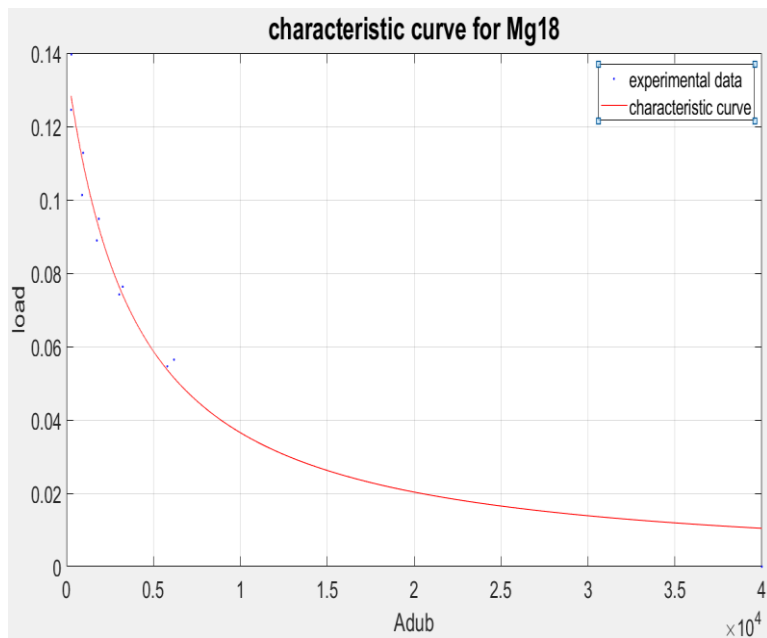
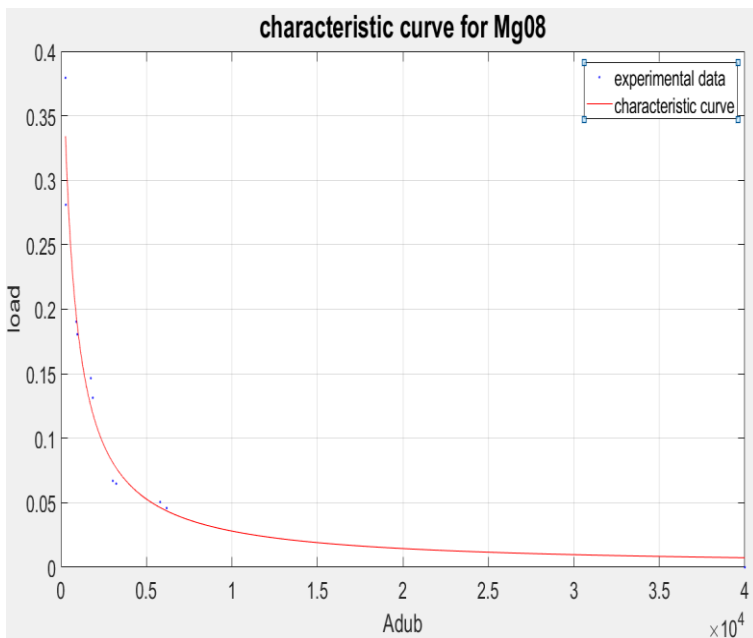


Figure 5.2 - Characteristic sorption curve for the samples

Sampling the characteristic curve it is possible to get the adsorption isotherms through the Polanyi theory, as explained in the paragraph 4.8. In the Figure 5.3 are presented the isotherms and also the experimental data at 30°C and 50° in order to give a measurement of the quality of the fitting.

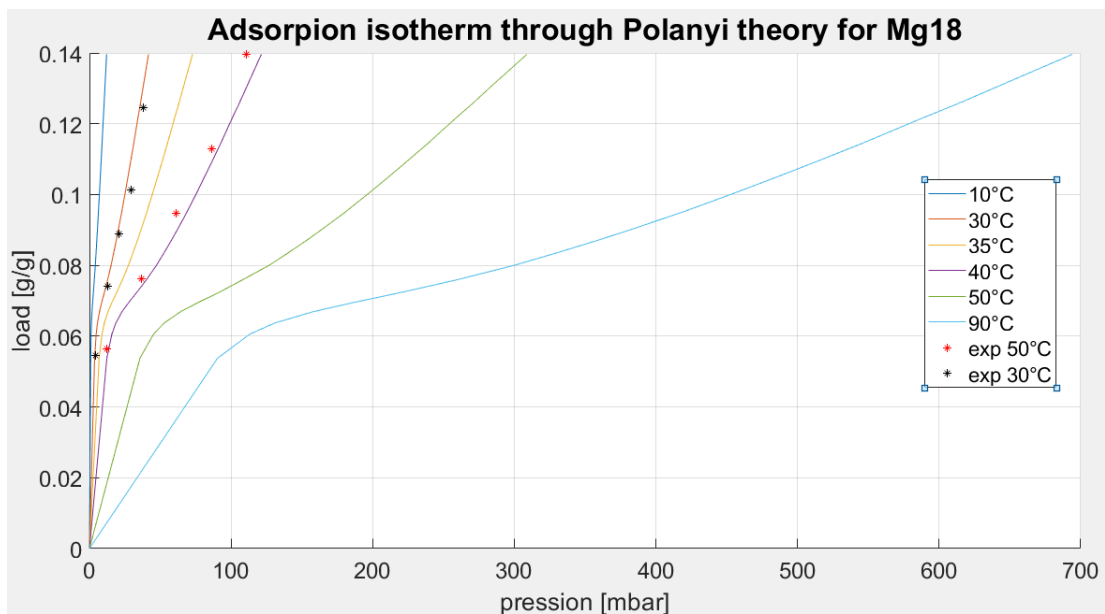
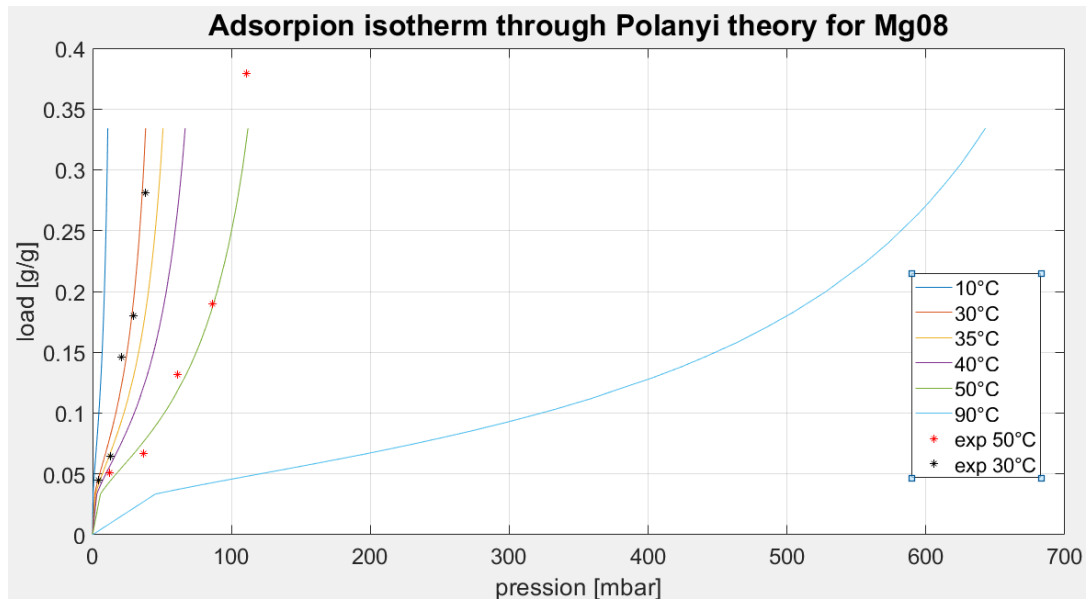


Figure 5.3 - Adsorption isotherms at 10°C, 30°C, 35°C, 40°C, 50°C, 90°C

Figures 5.4 show the thermodynamic cycle in the clapeyron chart, presented in the paragraph 4.8. It is important to point out that since the thermal boundary conditions are the same for the two samples and thus they rely on the same saturation pressure of water (i.e. the temperature in the winter and summer season, respectively 10°C and 30°C and accordingly the saturation pressure of water of about 12.3 mbar and 42.3 mbar), the isosteric heat that results is the same and equal to 56 KJ/mol.

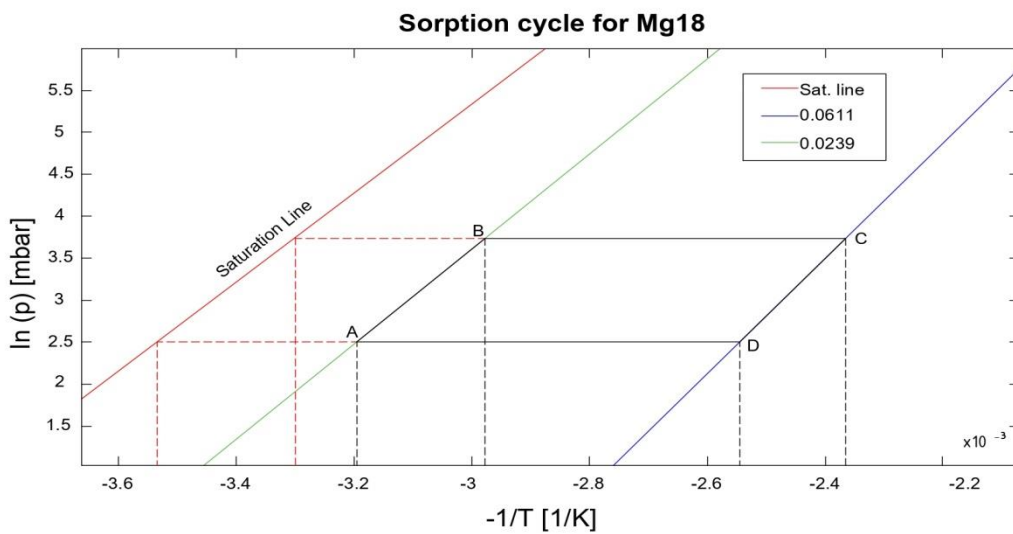
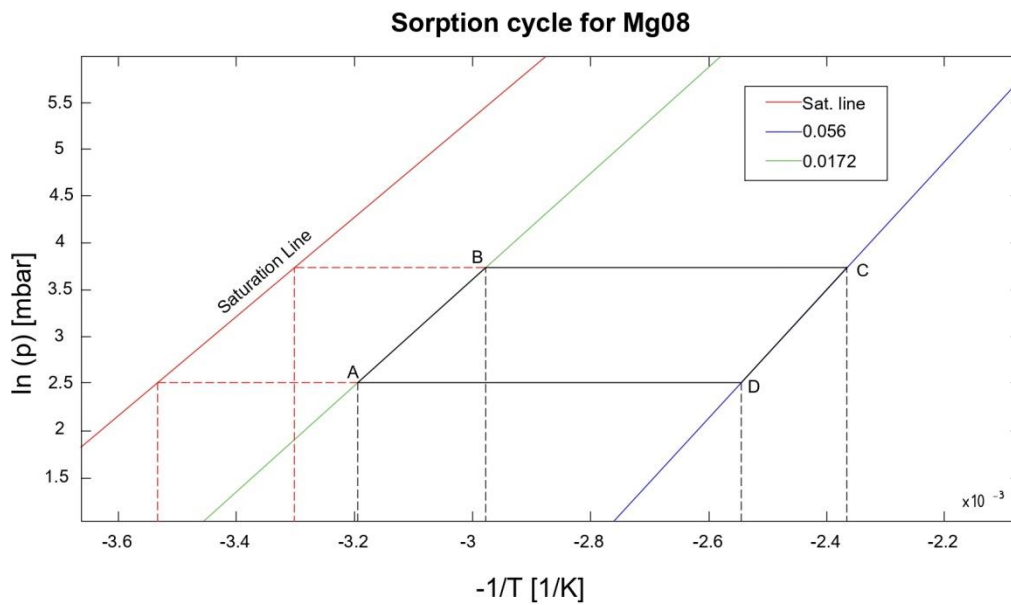


Figure 5.4 - Clapeyron cycle for the samples. Working temperatures:  $T_w=10^\circ\text{C}$ ;  $T_s=30^\circ\text{C}$ ;  $T_A=40^\circ\text{C}$ ;  $T_C=150^\circ\text{C}$

It is important to remark how the load variation  $\Delta x$  of both the cycles are significantly lower than the maximum one. This is due to the thermal constraints of the operating cycle, since it is not possible to decrease the appliance use temperature under a certain threshold, commonly in the range 30-40°C, which is the typical heat sink temperature needed to maintain a warm climate inside domestic house. On the other hand it is inappropriate to increase the charging temperature at levels higher than 150°C due to economic reasons, since it would require too expensive technologies to charge the material at higher temperatures, and due to limits in the salt  $MgSO_4$  itself. Indeed  $MgSO_4$  has a melting temperature of 52,5°C (16), lower than the desorption temperature, thus a risk of fusion of the salt is an additive problem. However this issue can be avoided by adopting smaller particles (< 200  $\mu m$ ), since it was experimented that the melt of  $MgSO_4$  occurs only for large particles.

In order to have a complete characterization of the material (Table 5.6), the cycled heat is calculated changing the operating conditions, in particular the charging temperature, assuming to work with traditional solar panels that reach a temperature of 90°C. As expected the adsorbed load decrease with the decreasing of the charging temperature and consequently the cycled heat resulted almost halved with respect to the one obtained when the maximum temperature is 150°C. Accordingly to the fact that the higher the charging temperature the higher is the adsorbed load, also decreasing the heat sink temperature ( $T_A$ ) it is experienced a rise in the load variation  $\Delta x$  and so an higher  $Q_u$ . As a matter of fact, the materials employed in the sorption heat applications are able to release much of their stored heat at low temperatures, thus having  $T_A$  close to the average  $T_w$  means higher cycled heat released.

	$T_A = 40^\circ C$		$T_C = 150^\circ C$	
	$\Delta x_A$	$\Delta x_C$	$q_{is}$	$Q_u$
	[g/g]	[g/g]	[KJ/mol]	[MJ/kg]
Mg18	0,0611	0,0239	56,9	0,117
Mg08	0,056	0,0172	56,9	0,122
	$T_A = 40^\circ C$		$T_C = 90^\circ C$	
Mg18	0,0611	0,041	50,4	0,0562
Mg08	0,056	0,032	50,4	0,067
	$T_A = 35^\circ C$		$T_C = 150^\circ C$	
Mg18	0,067	0,0239	56,9	0,136
Mg08	0,065	0,0172	56,9	0,15

Table 5.6 – Estimated sorption parameters

To have a complete characterization of the material the energy density is calculated, properties in which the composition of the sample plays a crucial role since the dry density influences the result. Obviously it is important to establish a good compromise between porosity and density, since one of the main challenge in the study of sorption application is to have the smallest portion of material to fit in the thermal storage systems that release as much heat as possible. In the Table 5.7 are reported the energy densities calculated when the boundary condition of the cycle are  $T_A=40^\circ\text{C}$  and  $T_C=150^\circ\text{C}$  and also the energy densities estimated in the preliminary thermal analysis.

	d	$E_d$ prel.	$E_d$
	[g/cm <sup>3</sup> ]	[GJ/m <sup>3</sup> ]	[GJ/m <sup>3</sup> ]
Mg18	1	0,037	0,117
Mg08	1,494	0,15	0,182268

Table 5.7 – Estimated energy density

It is evident the importance of the density of the sample, indeed Mg08 presents a very higher energy density with respect to Mg18, since it was loaded two times with a saturated solution of  $MgSO_4$  that provides an higher percentage of salt fraction inside the sample. It can be said that the preliminary thermal analysis produces consistent results since the energy densities estimated in that way are in the same range of that calculated with the climatic chamber. Moreover it is shown that the difference in terms of  $E_d$  between Mg08 and Mg18 is maintained in the two types of tests, confirming that the preliminary thermal test is valid for giving an impression of the most promising sample.

### 5.3.3 preliminary cost analysis

Lastly it can be worthwhile to evaluate the economic potential of the material developed, since one of the main purpose of this work is to elaborate a composite material that is economically advantageous with respect most of the already known material.

The KPI (key performance indicator) used for that aim is defined as the ratio between the price of the raw materials involved in the production  $C$  [€/ton] and the cycled heat  $Q_u$  [kWh/ton]:

$$KPI = \frac{C}{Q_u}$$

and it is measured in €/kWh.

The cost per ton of the raw materials is calculated considering that Portland cement price is on average 100 €/ton, while for anhydrous  $MgSO_4$  is about 160 €/ton. The cost  $C$  of the  $MgSO_4$  is calculated as follows:

$$C_{comp} = \frac{c_{salt}M_{salt} + c_{cem}M_{cem}}{M_{comp}}$$

Where with  $c_{salt}$  and  $c_{cem}$  are the prices in €/ton, while  $M_{salt}$ ,  $M_{cem}$  and  $M_{comp}$  is indicated respectively the mass of the salt, the mass of the cement and the mass of the dried material. Finally the cost of the samples resulted to be  $C_{comp}^{Mg18} = 139$  €/ton and  $C_{comp}^{Mg08} = 140$  €/ton, and consequently the price for stored kWh, considering  $Q_u$  calculated in paragraph 5.3.2, resulted to be  $KPI^{Mg18} = 4,27$  €/kWh and  $KPI^{Mg08} = 4,1$  €/kWh.

Since both samples are simply made of cement and  $MgSO_4$ , with a similar mass and with a cycled heat which varies only by a few units, the KPI in the 2 samples are nearly equal.

It is important to have a comparison between the sample here synthesized and the most employed sorbent. The table 5.8 shows the most useful thermal properties and the economic feasibility of the produced  $MgSO_4$ -based material in comparison with the characteristic of other sorbents identified in the literature.

As can be observed, under a point of view of cost per kWh, on one hand the samples produced with cement and  $MgSO_4$  are more efficient with respect to some of the most popular sorbents, like Zeolite 13X with  $MgSO_4$  or silica gel with  $CaCl_2$ , while on the other hand their performances are slightly far from those of material based on vermiculite and  $CaCl_2$ .

	Salt [%]	$T_C$ [K]	$E_d$ [GJ/m <sup>3</sup> ]	$C_{comp}$ [€/ton]	KPI €/kWh	Ref.
Mg18	65	150	0,117	139	4,27	
Mg08	67	150	0,182	140	4,13	
Zeolite 13X	/	160	0,72	2000	18,52	sorption thermal storage for solar
Silica gel		80	0,014	-	132	key
Zeolite13X/MgSO4	7,5	150	0,88	1343	13,1	sorption thermal storage for solar
Silica gel/CaCl2	33,7	90	0,76	3483	26,39	cementitius
Vermiculite+CaCl2		80	2,73	160	0,42	key
AIPO-18	-	90	-	100000	719	key
SAPO-34	-	95	-	100000	565	key

Table 5.8 – Comparison between the samples produced and other materials from literature in terms of KPI and energy density

## 6. Conclusion

Sorption heat storage has the potential to be one of the most promising technology able to move towards reliable and effective renewable energy sources in the next decades. The challenge of the scientific community is to identify a robust and low-cost sorbent material to be the foundation upon which build the future storage systems. The purpose of this thesis is to produce and examine a composite material based on Portland cement, one of the most available material in the world, in order to employ it in sorption thermal application. The choice fell on this material because is inexpensive and porous, characteristic that turn it in an ideal host matrix for hygroscopic salts. The combination of the matrix and the salt enhances heat and mass transfer, thus it is for these reasons that composite salt inside porous matrix (CSPM) materials are considered the most promising in the field of STES applications.

The hygroscopic salts chosen for this work are calcium chloride ( $CaCl_2$ ) and magnesium sulfate ( $MgSO_4$ ), considered from the literature and from recent researches among the best salts able to store and release heat under reasonable working conditions in heating applications. The composites are produced following two methods: a traditional dry impregnation a saturated solution of water and salt, and a novel in-situ approach, in which the slurry is created mixing directly the powder cement and the saturated solution. The advantage of this second method is that is possible to fill the host matrix with a higher concentration of salt with respect to the dry impregnation and the salt fraction inside the sample is thoroughly known.

After that, a preliminary thermal analysis was carried out with a simple calorimeter, which aim was to have a simplistic evaluation of the sample produced and to try to distinguish the most promising candidates in consideration of a STES application. Some considerations came to light: the in situ products experienced an higher energy density, probably due to the higher salt content in comparison with the impregnated ones, especially that synthesized with  $MgSO_4$ .

Among the samples with higher energy density, some of them were chosen to be further tested, this time in more specific way inside a climatic chamber in the National Institute of Metrological research: a pure in situ  $MgSO_4$ -based sample, a second in situ  $MgSO_4$ -based sample but with a double cycle of impregnation with the saturated solution of the same salt, and in the end an in situ  $CaCl_2$  also impregnated two times. The samples were loaded in the chamber with a flow of water vapor at 5 different level of relative humidity (RH) with the temperatures fixed (30°C and 50°C).

In this context the  $CaCl_2$ -based material proved to not be adequate for this kind of applications, since the salt spilled out from the matrix and damaged the sample when tested at 50°C and 50% RH. This is due to the high deliquescence rate of  $CaCl_2$ , that presents a low value of DRH (deliquescence relative humidity), thus having a high tendency to pass to the liquid state even at low RH and consequently putting the host matrix at risk to be altered or damaged. For this reason, and for the poor results in the preliminary thermal test, the  $CaCl_2$  samples were discarded and considered less promising than  $MgSO_4$  concerning this work.

Results from the sorption analysis in the climatic chamber about the samples with  $MgSO_4$  allowed to simulate a thermodynamic cycle in which typical operating condition of a heating system were applied. It was adopted solar collector panels able to collect radiations at  $150^\circ\text{C}$  and a temperature of the heat sink of  $40^\circ\text{C}$ , sufficient to maintain a warm climate inside a house room during the winter season. Through the thermodynamic cycle in a clapeyron chart, the most important thermal properties of the produced materials were obtained: isosteric heat, water uptake of the cycle, cycled heat and energy density.

At the end a preliminary cost analysis was conducted in order to estimate the cost per kWh and to compare it with the most widespread and known sorbent.

Both samples produced with  $MgSO_4$  provides a KPI of about 4 €/kWh, considering operating temperatures of  $150^\circ\text{C}$  and  $40^\circ\text{C}$  (respectively temperature of the panel and of the heating appliance as user). This estimated result, compared with values of KPI of other sorbents found in the literature, appears to be cheaper with respect the most of the others sorbents, with some exception, such as the vermiculite/ $CaCl_2$  based material that presents a lower value of €/kWh. Regarding the energy density potential, the obtained values of  $0,177\text{ GJ}/\text{m}^3$  and  $0.182\text{ GJ}/\text{m}^3$ , appears to be lower compared with better known materials like zeolite, thus the way to find an outstanding sorbent able to monopolize the market of STES applications is still problematic.

Nevertheless, the combined values of  $E_d$  and €/kWh are positively encouraging, the calculated KPI is small with respect the one of many sorbents employed in common sorption applications and the low-cost and porous structure of the cement can be exploited for a large number of combinations with different salts in the adsorption field.

# Bibliografia

1. F.Hassan, F. Jamil, A.Hussain. Recent advancements in latent heat phase change materials and their. 2022.
2. H. Ayaz, V. Chinnasamy, J. Yong, H. Cho. Review of Technologies and Recent Advances in Low-Temperature Sorption Thermal Storage Systems. 2021. <https://doi.org/10.3390/en14196052>.
3. V.H. Dalvi, S.V. Panse, J.B.Joshi. Solar thermal technologies as a bridge from fossil. 2015. <http://dx.doi.org/10.1038/nclimate2717>.
4. H.Mahon, D.O'Connor, D.Friedrich, B.Hughes. A review of thermal energy storage technologies for seasonal loops. 2021. <https://doi.org/10.1016/j.energy.2021.122207>.
5. Y.Tian, C.Y.Zhao. A review of solar collectors and thermal energy storage in solar thermal. 2012. <http://dx.doi.org/10.1016/j.apenergy.2012.11.051>.
6. L.Scapino, H.A.Zondag, J.Van Bael, J.Diriken, C.C.M.Rindt. Sorption heat storage for long-term low-temperature applications: A review on the advancements at material and prototype scale. 2016. <http://dx.doi.org/10.1016/j.apenergy.2016.12.148>.
7. A.Aduenko, A.Murray, J.L.Mendoza-Cortes. General Theory of Absorption in Porous Materials: Restricted. 2018. <http://dx.doi.org/10.1021/acsami.8b02033>.
8. K.S.W.Sing. Adsorption methods for the characterization of. 1998.
9. L.Scapino, H.A.Zondag, J.Van Bael, J.Dirinken, C.C.M.Rindt. Energy density and storage capacity cost comparison of conceptual solid. 2017. <http://dx.doi.org/10.1016/j.rser.2017.03.101>.
10. K.E.N'Tsoukpoe, H.Liu, N. Le Pierres, L.Luo. A review on long-term sorption solar energy storage. 2009. <http://dx.doi.org/10.1016/j.rser.2009.05.008>.
11. N. Yu, R.Z. Wang, L.W. Wang. Sorption thermal storage for solar energy. 2013. <http://dx.doi.org/10.1016/j.pecs.2013.05.004>.
12. N.C. Srivastava, I.W. Eames. A review of adsorbents and adsorbates in solid±vapour. 1997.
13. K.C.Ng, C.Y. Chung, H.T. Chua, C.H.Loke. Experimental investigation of the silica gel–water adsorption isotherm characteristics. 2001.
14. Stephen T. Wilson, Brent M. Lok, Celeste A. Messina,. Aluminophosphate molecular sieves: a new class of microporous crystalline inorganic solids. 1982. <http://doi/pdf/10.1021/ja00368a062>.
15. F.Trausel, A.De Jong, R.Cuyppers. A review on the properties of salt hydrates for thermochemical . 2014. <http://doi: 10.1016/j.egypro.2014.02.053> .
16. H. A. Zondag, J. Cot Gores, V. M. van Essen, M. Bakker. Characterization of MgSO4 Hydrate for Thermochemical Seasonal Heat Storage. 2009. <http://DOI: 10.1115/1.4000275>.
17. Adnan K. Salameh, Lynne S. Taylor. Deliquescence in Binary Mixtures. 2004. <http://DOI: 10.1007/s11095-005-1563-5>.

18. I.Lavagna, M.Pavese, D.Burlon, E.Chiavazzo, R.Risticò, V. Brancato, A. Frazzica. Cementitious composite materials for thermal energy storage applications: a preliminary characterization and theoretical analysis. 2020. <https://doi.org/10.1038/s41598-020-69502-0>.
19. J.X. Xu, T.X. Li, W. Chao, T.S. Yan, R.Z. Wang. High energy-density multi-form thermochemical energy storage. 2019. <https://doi.org/10.1016/j.energy.2019.07.076>.
20. Huijun Wu, Shengwei Wang, Dongsheng Zhu. Effects of impregnating variables on dynamic sorption characteristics and storage properties of composite sorbent for solar heat storage. 2007. <http://doi:10.1016/j.solener.2006.11.013>.
21. L.Aghemo, L.Lavagna, M.Pavese, E.Chiavazzo. Comparison of key performance indicators of sorbent materials for thermal energy storage with an economic focus. 2023. <https://doi.org/10.1016/j.ensm.2022.11.042>.
22. Yannan Zhang, Ruzhu Wang. Sorption thermal energy storage Concept, process, applications and perspectives. 2020. <https://doi.org/10.1016/j.ensm.2020.02.024>.
23. Andrea Frazzica, Angelo Freni. Adsorbent working pairs for solar thermal energy storage in buildings. 2017. <http://dx.doi.org/10.1016/j.renene.2016.09.047>.
24. What is cement? <https://civiltoday.com/civil-engineering-materials/cement/81-cement-definition-and-full-details>.
25. M.E.Boesch, S. Hellweg. Improvement Potentials in Cement Production with Life Cycle Assessment. 2010.
26. E.M.Gartner, J.F. Young, A.Damidot, I.Jawed. Hydration of portland cement.
27. Bleeding of Concrete: Causes, Effect and Ways to Reduce it. <https://happho.com/bleeding-concrete-causes-effect-ways-reduce/>.
28. Stephen Brunauer, P. H. Emmett and Edward Teller. Adsorption of Gases in Multimolecular Layers. 1938.
29. Kaps, K. Posern. Ch. Calorimetric studies of thermochemical heat storage materials based on mixtures of MgSO<sub>4</sub> and MgCl<sub>2</sub>. 2010. <http://doi:10.1016/j.tca.2010.02.009>.